

POLITECNICO DI TORINO

Corso di Laurea Magistrale
in Ingegneria Biomedica

Tesi di Laurea Magistrale
”Low Power Wireless Flexible
Piezoelectric Sensor for Non Invasive
Pulse Pressure Measure”



Relatori
Danilo DeMarchi
Paolo Motto Ros

Candidato
Gonzalo Pizarro

Anno Accademico 2019/2020

Abstract

Nowadays, systemic circulatory diseases are still one of the biggest challenges for the medical community to improve. Despite of the advances on diagnosis and treatments, the World Health Organization recognizes Ischemic Heart Disease as the principal cause of death for both sexes, at all ages and worldwide on a 2016's report.

Accordingly, there is a growing interest on providing better tools for the characterization of the state of the circulatory system exploiting the new trends such as wearable technologies and internet of things on medical devices.

The aim of this project was to develop a low power and wireless device for non-invasive measurements of the pulse pressure wave implementing a flexible sensor technology based on a piezoelectric material.

For this scope, an analog front-end circuit for the signal conditioning, and a microcontroller for the digital and transmission system were designed and integrated with the sensor. The system was tested by recording the pulse wave at the radial arterial pulse and sending the data to a personal computer while monitoring single performances at each stage.

In conclusion, the resulting prototype can accurately measure the pressure wave, digitalize it, and send it via Bluetooth, satisfying the design requirements. In addition, the design can serve as a model for a further development that extends its functions, in which pulse wave analysis and processing is applied.

Acknowledgements

I would like to acknowledge all the people that has accompanied me on the long way throughout this process.

First, to my family for all the support all these years and in particular to my mother that always believed in me. Without her i would not be where i am. Also, my special regards to all my friends that made this journey so pleasant.

Finally, I wish to show my gratitude to all the team of LIADE in the UNC for the invaluable experience and for give me the opportunity of do my first steps on the field. Thanks to Ricardo Taborda professor, neighbour and friend. And thanks to Sara, i could not go so far without her unconditional support.

Contents

1	Introduction	7
1.1	Circulatory System	7
1.1.1	Components	8
1.1.2	Blood Flow	9
1.1.3	Pulse Pressure	10
1.1.4	Factors that affect Pulse Wave	11
1.1.5	Pulse Wave Transmission	12
1.1.6	Pulse Wave Measuring	13
1.2	Piezoelectric Materials	14
1.3	Flexible Circuits	15
1.3.1	Substrates	15
1.3.2	Single Sided Flexible Circuits	16
1.4	Signal Conditioning	17
1.4.1	Amplification	18
1.4.2	Noise	19
1.4.3	Filtering	20
1.5	Real Time Operating Systems (RTOS)	23
1.6	Bluetooth Low Energy (BLE)	24
2	Materials and Methods	25
2.1	Piezoelectric Transducer	25
2.2	Analog Front End Overview	28
2.3	Voltage Supply	28
2.4	Charge Amplifier	29
2.4.1	Component selection	31
2.5	Low Pass Filter	35
2.6	High Pass Filter	41
2.7	Band Pass Filter	43
2.8	Microcontroller	45
2.8.1	ADC	47
2.8.2	BLE	49

2.8.3	Deep Sleep	50
2.8.4	Firmware	51
2.8.5	MATLAB script	53
3	Results	55
3.1	Charge Amplifier	55
3.2	Low Pass Filter	56
3.3	High Pass Filter	58
3.4	Band Pass Filter	60
3.5	ADC Sampling	60
3.5.1	Power Consumption	62
3.5.2	Pulse Wave Recording	65
4	Conclusion	67

List of Figures

1.1	Central and Peripheral Circulation	8
1.2	Pulse Wave	10
1.3	Abnormal Pulse Wave	11
1.4	Pulse wave transmission	13
1.5	Piezoelectric Effect	15
1.6	Single Sided Flexible Circuit	17
1.7	Operational Amplifier equivalent circuit	18
1.8	Random White noise	20
1.9	Filter types	21
1.10	Real vs Ideal Filter Response	22
2.1	Sensor Composition	26
2.2	Sensors Out	27
2.3	Sensor model	28
2.4	Voltage Reference	29
2.5	Charge Amplifier	30
2.6	PCB 3D View	33
2.7	Low Pass Frequency Response	36
2.8	Low Pass Filter	37
2.9	Radial Pulse Wave	38
2.10	Carotid Pulse Wave	38
2.11	Carotid and Radial PSD	39
2.12	Low Pass Frequency Response	40
2.13	Low Pass Filter	41
2.14	High Pass Frequency Response	42
2.15	High Pass Filter	43
2.16	Band Pass Frequency Response	44
2.17	Band Pass Frequency Response	45
2.18	Apollo3 Evaluation Board	47
2.19	ADC block diagram	48
2.20	BLE module block diagram	50
2.21	MATLAB script flow diagram	54

3.1	Test Circuit	55
3.2	Impulse	56
3.3	Low Pass response comparative	58
3.4	Band Pass Filter - Measured	60
3.5	Sine Wave vs ADC Wave	62
3.6	Power Measurement Circuit	63
3.7	Recorded Wave	65
3.8	Recorded Wave PSD	66

List of Tables

2.1	Op amp comparison table 1	31
2.2	Op amp comparison table 2	32
2.3	Op amp comparison table 3	32
2.4	Op amp comparison table 4	32
2.5	Op amp comparison table 5	33
2.6	Op amp comparison table 6	34
2.7	Op amp comparison table 7	34
2.8	Op amp comparison table 8	34
2.9	BLE MCU comparison	46
2.10	Core Architecture MCU comparison	46
2.11	Power Consumption MCU comparison	46
2.12	ADC MCU comparison	47
3.1	ADC sampling performance	62
3.2	Power Consumption from data sheet	64

Chapter 1

Introduction

Early detection of cardiovascular diseases is one of the most important usages for pulse wave monitoring. The convenience non invasive technique makes it extremely suitable for widely use at community levels. Factors derived from pulse wave analysis have been used to detect hypertension, coronary artery diseases. For example, losing the diastolic component is the result of reduced compliance of arteries. (Cohn 1995) Pulse wave is suggested to be early marker for those diseases and guide for health care professions during the therapy.

The goal of this work was to develop a first prototype of a device capable of measure the pulse wave implementing a flexible piezoelectric transducer. The gadget consists of an embedded system that produces a signal from the wave generated superficially on the pulse and its capable to send it wireless, by Bluetooth. In addition, the design aims to maximum size reduction as result of high integration of the components in order to make it wearable. Also, it is optimized on power consumption, longing the battery life.

This first chapter introduces some theoretical concepts that guides the reader with a background on the case of study. First, relevant physiology of the circulatory system is briefly described as well as characteristics of the pulse wave. Then, some important terms of the electronic aspect such as signal conditioning are presented.

1.1 Circulatory System

The circulatory system is a complex structure composed of a pump, the hearth, and a vast network of vessels, the arteries and veins, in which blood

can travel through the hole body to service the needs of the tissues, such as, nutrients exchange or waste products and hormones transport, while helps to maintain an adequate physiological environment.

On his way out of the hearth the blood is first forced to pass across the lungs for the exchange of oxygen in place of carbon dioxide due to the primer systolic discharge and then once the gas trade is done, the blood is pumped to the rest of the body. Consequently, is possible to separate two principal circulation paths: the pulmonary circulation and the systemic circulation.

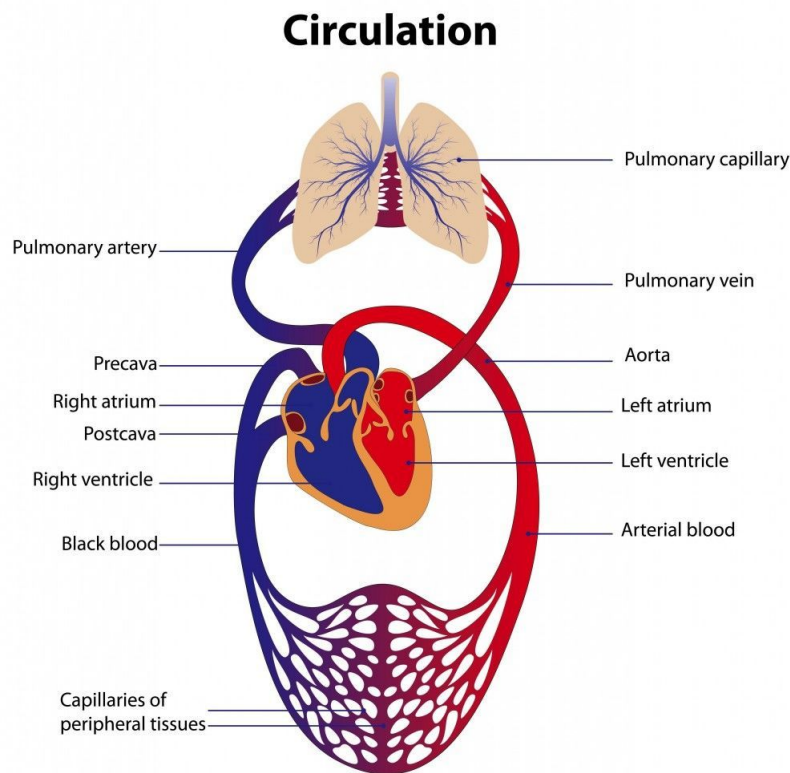


Figure 1.1: Central and Peripheral Circulation

1.1.1 Components

The systemic circulation is first composed of a hierarchical tree of arteries, next it divides in arterioles and therefore in capillaries. Once the flow arrives to the organs, needs to come back to the hearth and begins to converge again in venules and veins.

Each vessel has a structure due to its function:

- Arteries: are vessels in which the blood flows rapidly, presenting a strong and elastic tissue layer in order to hold up the highest pressures within the system.
- Arterioles: they are capable of regulate the flow in response of the needs of the tissue. Accordingly, their have a strong muscular wall that can control the lumen.
- Capillaries: they are the smallest vascular elements of the system. Present thin layers with pores in which all the substances as nutrients and hormones are exchanged.
- Venules: collect blood from capillaries while gradually grow on larger vessels.
- Veins: blood travels across them to the hearth. Present a thin wall because of the low pressure

The arterial stiffness is the first vessels modification, responsible for several pathological processes, which can lead to cardio vascular diseases. For this reason, the arterial elastic properties are used for risk stratification purposes in several populations.

Recently, the European Society of Cardiology guidelines for the management of arterial hypertension suggested the measurement of PWV, considered the gold standard method for assessing arterial stiffness, as a tool to evaluate the arterial system damage, vascular adaptation, and therapeutic efficacy [6].

1.1.2 Blood Flow

In simple words, blood flow is the volume of blood moving through a vessel at any time. The blood displacement is a result of a pressure gradient, the difference between the force generated by the heart at each beat that pushes it forward and the resistance of the vessel that opposes the flow.

This leads to a relation called Ohm's Law:

$$F = \frac{\Delta P}{R}$$

However, changes on pressure generate a distension of the vessels walls decreasing their resistance. Hence, flow can raise more than expected due to the summed effect.

Owing to the pulsatile nature of the hearth the arterial blood pressure is not constant. Therefore, it oscillates between systolic and diastolic values giving origin to the pulse pressure.

1.1.3 Pulse Pressure

Normally, when the flow exits the aorta, the pressure will raise to above 120mmHg and then it decreases to a minimum of 80mmHg. This difference between the peaks is called pulse pressure.

Pulse can be recorded to a set of time series data and represented as a digraph which is called pulse waveform or pulse wave for short.

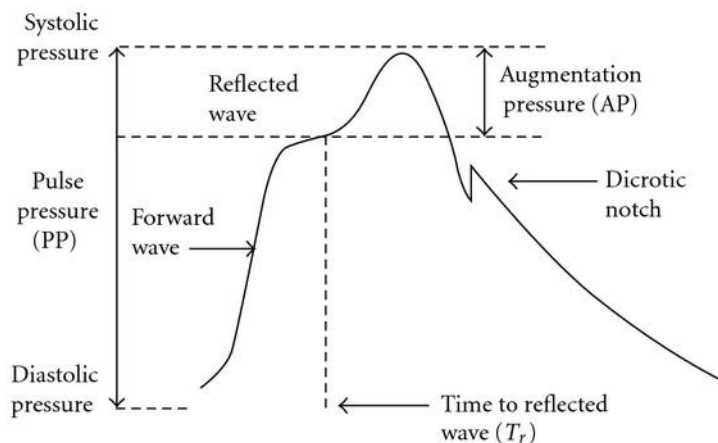


Figure 1.2: Pulse Wave

Spite of its simplicity, this wave carries with it a big set of valuable information for being mainly influenced by the distensibility of the arterial tree and the volume of blood ejected by the hearth. A greater volume results in a higher-pressure difference. At the same time, more rigid arteries will need a higher pressure for the same flow, rising the gradient though.

Pulse waveform characteristics, such as the shape, the intensity, the velocity and the rhythm are closely bound up with cardiovascular function. In particular, the pulse wave evidences the state of the circulatory system, since, its morphology depends on the interaction of the left ventricle and the physical properties of the arterial circulation.

Hence, measuring it can be a useful tool for cardiovascular disease control. For example, diagnosis of hypertension is done thanks to detection of elevated pulse pressure segments, as well as, in patients with cardiac failure or diabetes mellitus the treatments are supported by interpretation of the wave.

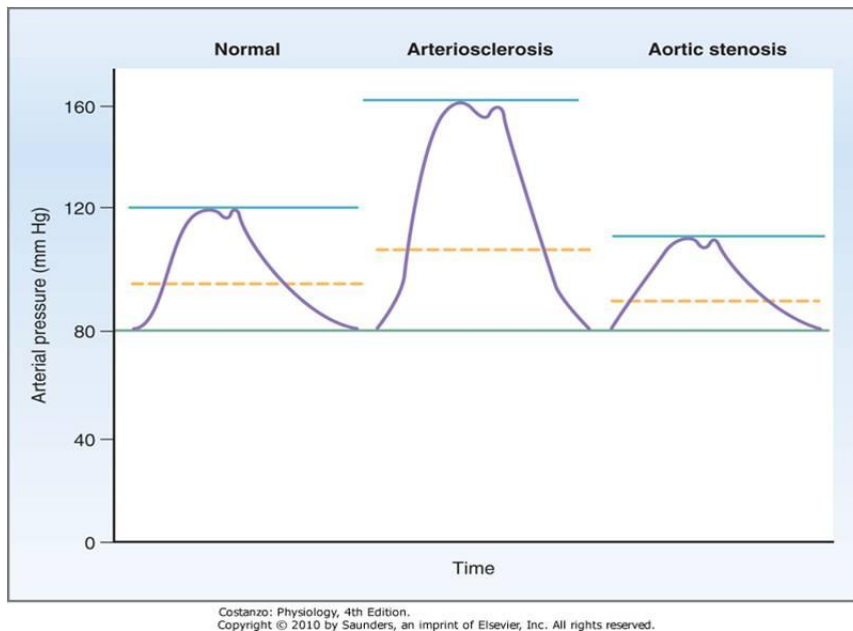


Figure 1.3: Abnormal Pulse Wave

1.1.4 Factors that affect Pulse Wave

- Ageing: on normal subjects the more remarkable changes are, first, a notably trend of presenting a bigger systolic peak in older patients, and second, the partial or total absence of the second diastolic wave. The augmented peak is reasonably attributed to arterial stiffness that leads to a higher pressure.
- Physical fitness: studies on patients that regular do exercise evidence a less augmentation on the pulse wave that would be explained as a result of improvement on endothelial function.

- Food: due to ingestion of food, and therefore ulterior insulin release changes on the contour of the wave can be observed
- Heart Rate: because of its nature, the wave can sudden important changes in its shape due to heart rate variations. For instance, a slower heart rate leads to an increased pulse pressure because of the summation of the incident and reflected wave on a larger period for ventricular ejection.

1.1.5 Pulse Wave Transmission

The pulse wave generated by the pumping will travel along the hole system. First, the impulse at the aorta overcomes the inertia of the blood and moves forward, until reaches the periphery where is reflected. As a result, the final waveform is composed of both primary and secondary waves.

The wave intensity falls while the vessel become smaller as a result of vessel damping. This phenomenon it related to the resistance to the flow and the distensibility of the vessel.

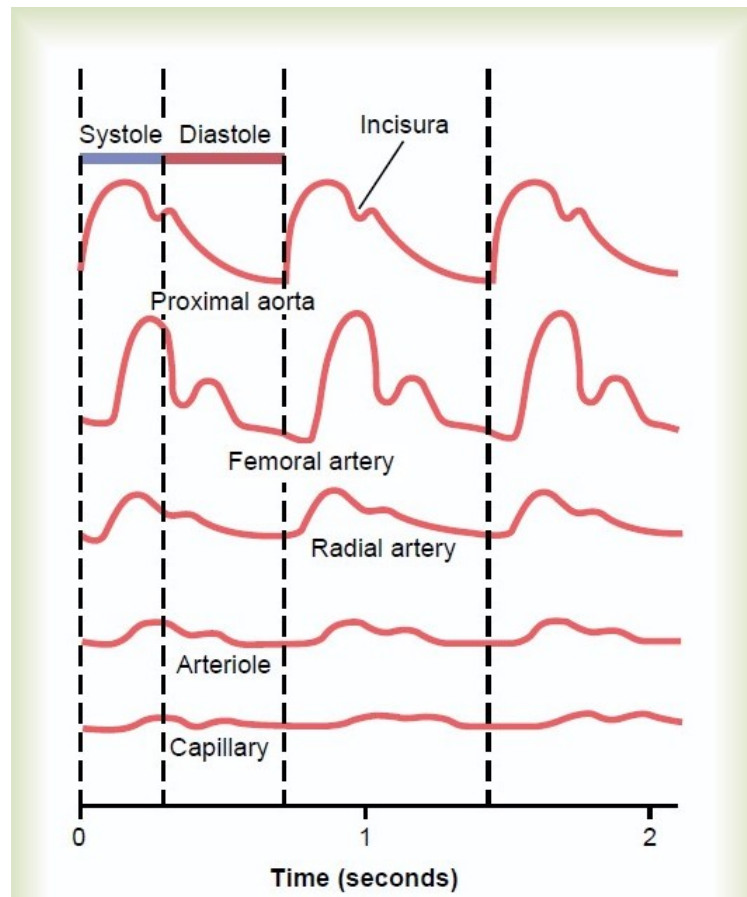


Figure 1.4: Pulse wave transmission

Despite of being initiated at the aorta, the same qualitative information of the pulse wave can be measured at the radial artery with non-invasive methods, providing a safer, quicker, and simpler alternative that helps to the diagnosis and treatment of several cardiovascular diseases. For instance, a notably parameter such as the duration of the systole and diastole can be measured with no significant difference with the one at aortic level.

1.1.6 Pulse Wave Measuring

The pulse wave can be measured using several approaches depending on three principal diverse physical properties:

- Pressure Pulse: the pressure pulse wave is generally measured with a finger cuff or another pressure device capable of perform applanation

tonometry. The technique consists in recording the response to compression of an artery with a pressure sensor. Despite of being regularly done at the eyeball with the highest fidelity it can also be done at the wrist or other parts but it is always limited by the presence of the tissue. For this reason, calibration is needed.

- Volume Pulse: when it comes to volume changes within the body, plethysmography is mostly used. It consists of detection of the blood flow by measuring pressure differences across a limb. However, a more sensitive method is the photoplethysmography. A simple superficial measurement that takes advantage of differences in optic properties of the tissues and blood. In fact, it emits an infrared light (IR) that its mostly absorbed by the blood flow, allowing to detect changes in it similar to pulse oximetry.
- Flow Pulse: Finally, flow measurements are principally done by Doppler ultrasound sensors.

1.2 Piezoelectric Materials

A piezoelectric sensor is constructed with a piezoelectric material. Basically, is a material that produces an electric charge due to a mechanical stimulus, or vice versa, it can be electrically stimulated to produce mechanical movement.

From one hand, direct piezoelectric effect is due to a reorganization of the internal structure of the material once it has been stressed. The applied forces displace the atoms and thus, electrical dipoles are formed. In consequence, the material is no more electrically neutral.

On the other hand, when the material is electrically stimulated, for example with an external electric field, a mechanical strain is induced as a result of changes in the internal structure.

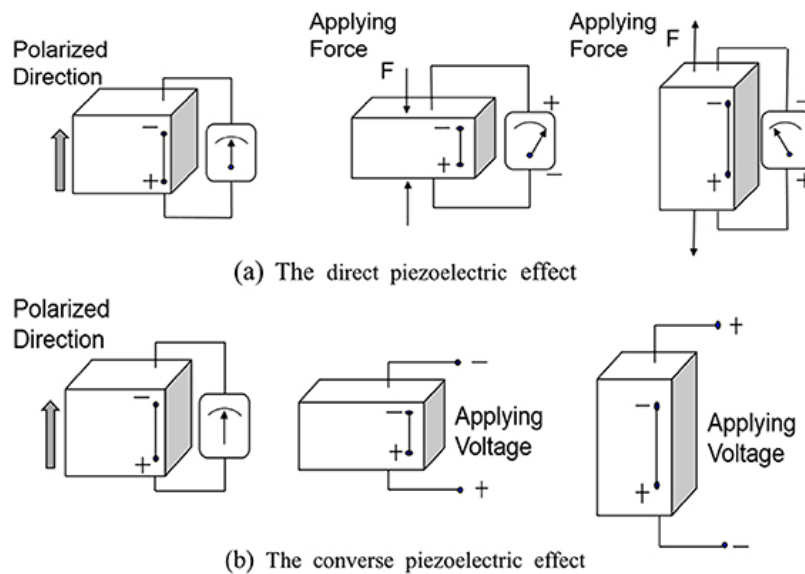


Figure 1.5: Piezoelectric Effect

1.3 Flexible Circuits

Flexible circuits are a special type of electronic circuit that can be deformed while maintaining functional integrity. Several degrees of flexibility can be reached depending on the technology and the manufacturing process, however they are usually clustered in: bendable or roll-able, permanently shaped and elastically stretchable.

While very complex structures can be done with this kind of technology, on its most essential level involves a conductor trace surrounded by an insulator film. Besides its mechanical differences with conventional rigid circuits, they can also present advantages on manufacture issues, such as, assembly time or total volume reduction. In fact, for the same design, a reduction of about 70 can be achieved when implementing with flexible wires rather than its rigid version.

1.3.1 Substrates

Nowadays, there three materials available for flexible electronics manufacturing:

- Polymers

- Glass
- Metals

The metal foil is flexible and sustain high temperature, although, is limited on the freedom of design and is high cost. Glass can actually be considered for flexible electronics applications because, when fabricated with a thickness less off 200 μm , it is relatively bendable.

’ Unfortunately, the application space open to thin glass is likely to be small because this material is still brittle, difficult to produce in large sheets, and unsuitable for R2R processing.

Regarding the mechanical properties, polymer materials are the best suited for flexion stress but the low fusion temperature compared to metals makes them no compatible to a wide range of processes, limiting the temperature to no more than 150 °C. However, is possible to find adequate polymers that can respond to the required optical properties, surface roughness and thermo-mechanical properties for the application. Some of the most often implemented polymers include:

- Thermoplastic Semi crystalline Polymers such as polyethylene terephthalate (PET) and polyethylene naphthalate (PEN)
- Thermoplastic Non-crystalline Polymers: polycarbonate (PC) and polyether-sulphone (PES)
- High Tg Polymers: polyarylates (PAR), polycycloolefin (PCO), and polyimide (PI).

1.3.2 Single Sided Flexible Circuits

Single sided refers to the simplest manufacturing flexible circuit type. Generally used for point to point wiring, each track of conductor is surrounded with an insulator layer and an adhesive that bonds it to the flexible substrate.

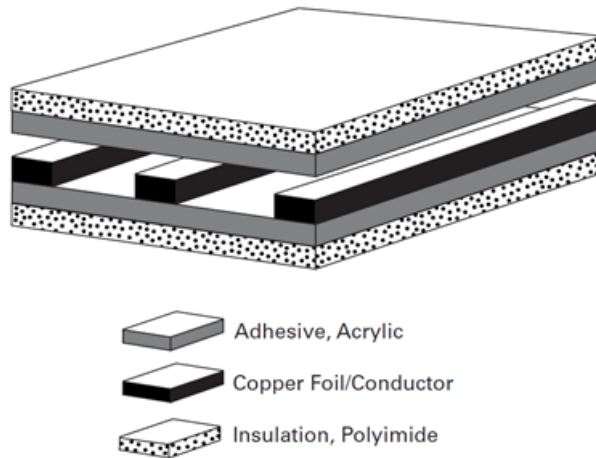


Figure 1.6: Single Sided Flexible Circuit

1.4 Signal Conditioning

Nowadays, sensors and transducers are found as a part of almost any electronic circuit that is designed with the scope of measuring some physical property, such as temperature, pressure, flow, etc.

A sensor is a device that responds with an electric signal when stimulated, whereas, a transducer, can transform the original form of energy that excites it into another. Despite this difference, both terms are generally accepted as equal.

Commonly, a sensor will be putted together with a system that modifies its output in order to make it compatible with a digital system. In fact, a raw electrical signal from a sensor would need a series of transformations such as:

- Amplification
- Level translation
- Galvanic isolation
- Impedance transformation
- Linearisation
- Filtering.

Next, the principal and more relevant operations for the study case are discussed.

1.4.1 Amplification

Amplification of a signal is the operation of increasing its magnitude of a desired quantity denominated as Gain. Usually, sensors produce a level voltage, current or resistance change that are modulated with an operational amplifier.

The operational amplifier, in short op-amp, is an electronic device capable of achieve a very high amplification, this is, more than 100000 times of its input value. It is a differential input, single ended output amplifier in which its operation is defined by the closed loop created between the output and the inverting or the non inverting input.

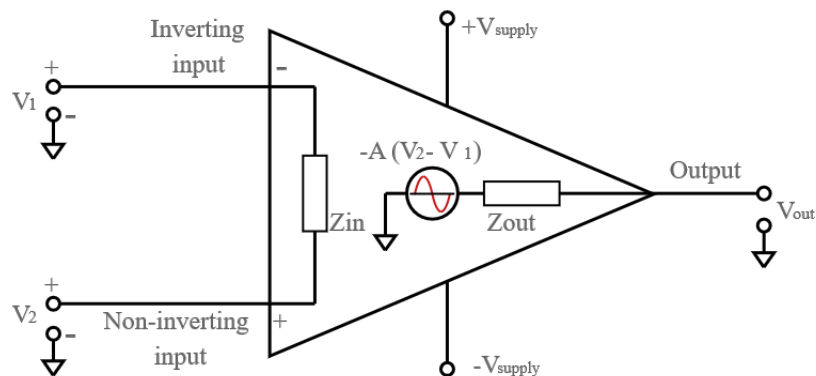


Figure 1.7: Operational Amplifier equivalent circuit

Ideally, op amps will present infinite gain for differential input signals meanwhile the common signals will be totally rejected. Also, the voltage output will be zero when the circuit is not excited by a signal, this is, a 0V offset voltage. A 0V difference of potential will be found at both inputs due to 0A input bias current. However, real life devices have practical limitations that can strongly affect the performance for a particular application.

Most of op Amps circuits will be sensible to one of the following parameters:

- Input Offset Voltage: normally, fabrication processes will lead to internal mismatches in the amplifier structure. Thus, a small voltage, such as some mV or μV in some cases, is present on the output in order to

balance the difference between the inverting and non inverting output. Generally, JFET and CMOS are more prone to present higher offset values than BJET op amps. This value is mostly important when DC accuracy is required.

- Input Current: both, the inverting and the non inverting inputs will drain some amount of current when the op amp will be active. As a result, the input bias current is calculated as the average of the two currents:

$$I_b = \frac{I_N + I_P}{2}$$

In this case, BJET op amps present higher input bias current than CMOS and JFET devices. If the source impedance is high, then, the output signal will be lower due to the load of the source by the input bias current.

1.4.2 Noise

Noise can be defined as any unwanted disturbance that interferes with a signal of interest and it involves a huge spectrum of fields of interest. Next, the noise present in a circuit is briefly introduced.

Practically, all measured signals are corrupted with some level of noise and the performance of the circuit can be drastically degraded if no rejection operations are applied to it. First, two big groups distinguish noise origin, internal noise and external noise.

Electronic circuits are sensible to interact with external sources of noise such as electric, magnetic, electromagnetic or also electromechanical. This phenomenon is mainly a consequence of parasitic capacitance and mutual inductance between other closer circuits or even between adjacent parts of the same circuit. Also, conversely to ideal models any conductor within the circuit will act as a small antenna. Nevertheless, other paths such as ground and power supply buses can be a noise source too.

Depending on the source, different strategies can lead to effective external noise reduction, for instance:

- Filtering
- Decoupling

- Guarding
- Shielding
- Ground loop elimination

On the other hand, internal or inherent noise, is a random process that affects every circuit even though external noise was not present or totally rejected. The most common form of it is the thermal noise present in resistors due to random electron movement. As electrons move within the resistor they generate little currents with random intensity and direction that at each instant of time generate a voltage across it. As a result, a random fluctuation of the elements voltage is always present, even if it is not connected to a net in a circuit. However, considering that non ideal capacitors and inductors have their own resistance, thermal noise is present on all passive elements.

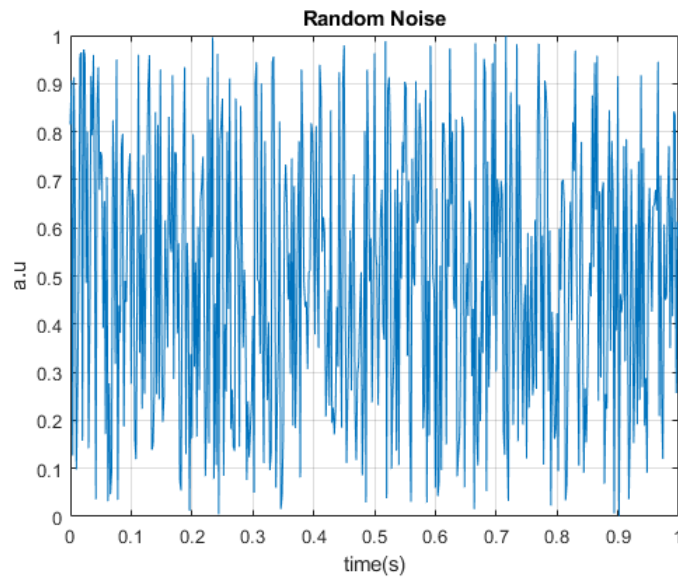


Figure 1.8: Random White noise

1.4.3 Filtering

As discussed before, noise reduction is a fundamental procedure in a design process. Filtering, refers to remove of some unwanted signal component at the output of a circuit while the signal of interest has a minimum intensity reduction. Depending on its nature, filters can be analogue or digital while depending on its components it can be active or passive. For this case of

study analogue active filters are discussed which are composed of operational amplifiers, resistors and capacitors.

In order to analyse filters effects, the input and output signals are evaluated on the frequency domain as gain versus frequency and phase versus frequency diagrams. The relation between the output and the input on the frequency domain is normally called Transfer function or Frequency Response $H(s)$:

$$H(s) = \frac{V_o(s)}{V_{in}(s)}$$

There are several different filter types:

- Low-Pass
- High-Pass
- Band-Pass
- Band-Reject

Low Pass filters are designed for reduction of all frequencies beyond a critical frequency denominated cut off frequency. As its name evidences, all lower frequencies can pass unaffected through the filter. In contrast, High Pass filters respond on a opposite way by targeting all higher frequencies from the cut off frequency. When combined, a Band Pass filter is formed by letting a band of frequencies between both, high pass and low pass cut off frequencies unaffected whereas a band rejection, or notch filter is able to keep out of the system a well defined set of them.

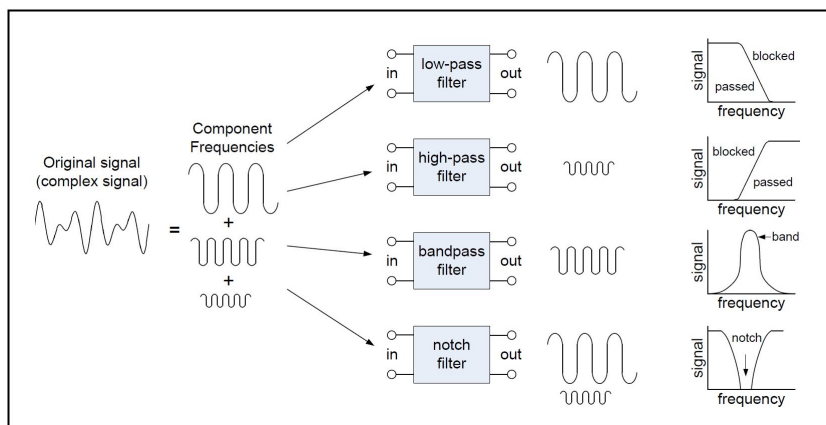


Figure 1.9: Filter types

While ideally a filter should totally reject the desired range of frequencies, real filters, as every component, has physical limitations. For this reason, how much the filters response gets close to the ideal depends on several parameters that directly affect the design, and strongly depends on the application requirements.

These are:

- Order: naturally, the higher the the order, the fast the slope of the filter. It is proportional to the number of components in the implementation and because of this as the order increases the filter becomes bigger, more complex, and more costly.
- Roll-off: it is a rate that evidences how much the signal diminishes in a defined interval of frequencies, normally, expressed in dB/dec or dB/octave.
- Amax: represents the maximum amplitude variation in the passband.
- Amin: is the minimal gain the attenuated signal will present in the stopband.
- f_1 : is the cut-off frequency and its equal to the frequency in which the signal's amplitude is reduced to a -3dB magnitude. This is, almost the half of its input value.
- f_s : is the start point of the stop band.

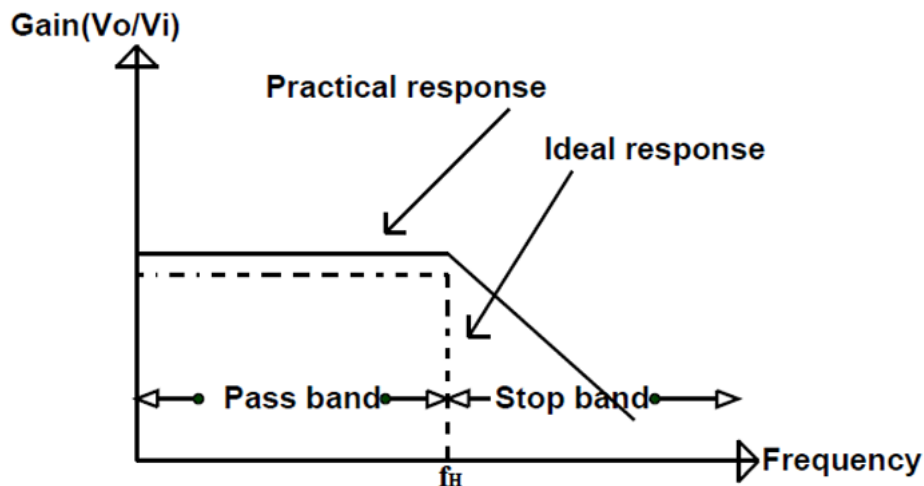


Figure 1.10: Real vs Ideal Filter Response

1.5 Real Time Operating Systems (RTOS)

A real time operating embedded system can be considered as a system that ensures a response within a time deadline.

Basically, there are two types of time requirements in a embedded application: Hard Real Time and Soft Real Time.

In the first case, the time interval in which the systems active response is needed is critical, and therefore a lack of it ports to a total failure of the system. For illustration, an electronic break with a delayed response.

On the other side, a soft real time violation still preserves the utility of the system, such as, an screen in which the refresh rate is slow will be annoying rather than, totally useless or critical.

On embedded applications one of the most suitable options for development is the Free RTOS kernel, which is a free kernel that manages the program flow and tasks in order to accomplish the hard time requirements of the system. In this paradigm, the application can be seen as a set of independent programs, each of it is known as a thread or task. Normally, only one task is capable to run at time so the tasks present an execution priority that allows the scheduler decide which one has to be running.

In summary, most of the benefits are:

- Abstracting away timing information
- Maintainability/Extensibility
- Modularity
- Team development
- Easier testing
- Code reuse
- Improved efficiency
- Idle time
- Power Management

- Flexible interrupt handling
- Mixed processing requirements

1.6 Bluetooth Low Energy (BLE)

Bluetooth low energy was born as a complete new version of its predecessor, classic Bluetooth, with a different paradigm based on a design that intended to make a new low power, low cost, low bandwidth and low complexity standard. Nowadays, most of BLE applications are running on coin cell powered systems, showing how this smart version can drastically enhance energy efficiency in several products, in particular wearable devices.

First, when it comes to connection between devices, BLE, supports two ways of communication : broadcasting or connection.

Broadcasting is the simpler way a device can send data through the BLE specification, it means a device will continuously send unidirectional data and any scanning near device can receive it. As a result we can define two different roles: the broadcaster, the peer who sends the data, and the observer, the "listening" device that acts as receiver. The most important feature of this mode is that in absence of a direct connection, the broadcaster is capable of data transfer to several devices at the same time.

In a more complex way, a connection is needed when two devices have to exchange data reciprocally. When is accomplished, data can travel bidirectionally while remains private thanks to impossibility of other devices to being part of the connection itself. In contrast to broadcasting, two different roles can be assumed in a connection: A central role, which scans and initiates a connection. Then, schedules the connection times and the data exchanges. Or, a peripheral role, that once it accepts the connection is guided from the central peer for data transfer.

Chapter 2

Materials and Methods

2.1 Piezoelectric Transducer

The transducer is made up of several layers that contain the active piezoelectric material and the electrodes, developed on a Kapton substrate. The electrodes are composed of molybdenum (Mo), whereas the sensing element is constituted of aluminium nitride (AlN). The flexible substrate follows the sensor expansion and contraction, that generates the charge proportional to the stress due to the direct piezoelectric effect.

In addition, some characteristics are presented:

- Active area: 4 x 5mm²
- Thickness: 1 μ m
- Capacity: (3 – 3.5nF)
- Impedance: (40 – 60k Ω)
- Current: nA range

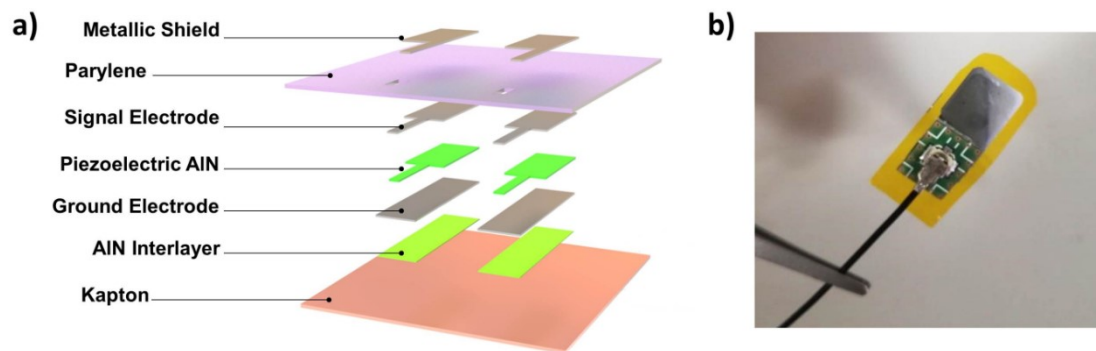


Figure 2.1: Sensor Composition

On the other hand, the IIT researchers were measuring the sensors output with a four channels charge amplifier with the following characteristics:

- Gain: -227mV/pC
- 1st Order Low Pass filter with f_c at 482Hz
- 1st Order High Pass filter with f_c at 0.5Hz
- Device: AD8606

And the resulting wave while measuring the pulse wave at carotid level:

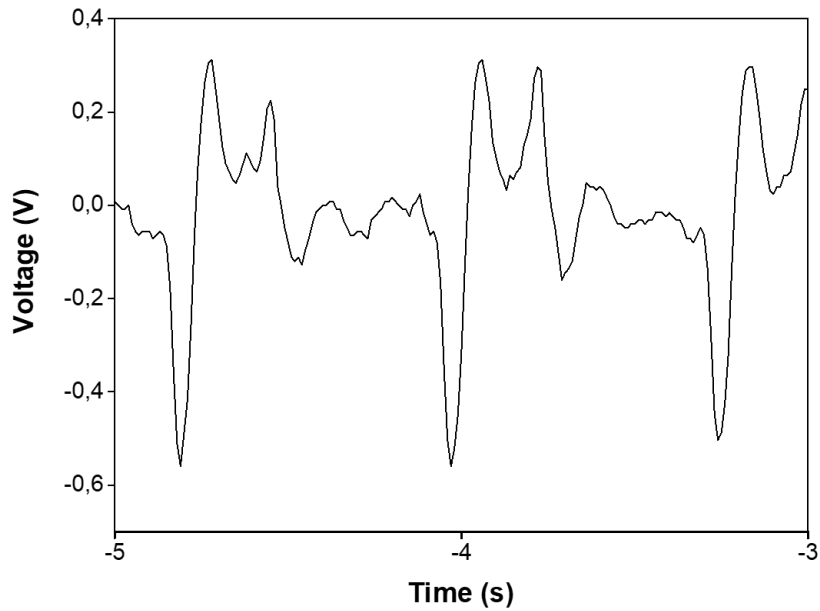


Figure 2.2: Sensors Out

In order to simulate the behaviour of the sensor, first, it was modelled. Considering it connected to a circuit, the generated charges will flow in, producing a current so primary it can be modelled as a current source. Next, a parallel capacitor can be added due to effect of the electrodes and finally a parallel resistor is added that simulates the discharges.

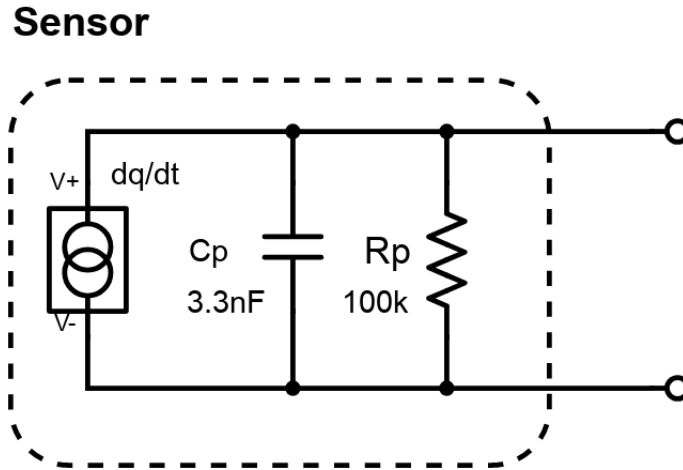


Figure 2.3: Sensor model

2.2 Analog Front End Overview

Above all there is a signal conditioner system that amplifies and filters the signal generated by the sensor. This first stage adjusts the voltage levels for the microprocessor and its composed of a pre-amplifier and a band pass filter made with a low pass filter and a high pass filter in cascade.

They are all single supply circuits, powered with a V_{cc} voltage of 2.5V with the reference set at $V_{cc}/2$, 1.25V allowing to preserve the dynamic range of the signal.

The passive components in the filters where designed taking into consideration power consumption, size and noise. Hence, resistors where chosen with a value in the order of kilo ohms. Consequently, the capacitors where calculated.

2.3 Voltage Supply

As the system is conceived for a single battery supply, a 3.6V TL2450 battery with a 500mAh capacity was used for the tests. However, the V_{cc} supply of 2.5V was derived from an ultra low current voltage regulator, the Linear Technologies LT6656. Regarding the V_{ref} of 1.25V it was derived from another op Amp considering that the most convenient packaging of the solution

for the design holds 4 channels where two are used for the filtering and one for the amplifier. In consequence, the free last one was then implemented as a voltage reference.

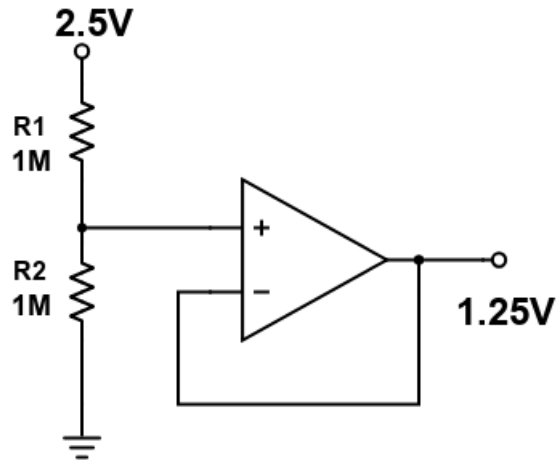


Figure 2.4: Voltage Reference

2.4 Charge Amplifier

Firstly, a pre-amplifier converts the charge output of the sensor in voltage. The feedback capacitor is charged with the same charge present at the inverting input of the operational amplifier, transducing it in a voltage while the feedback resistor is placed to avoid the op amp saturation.

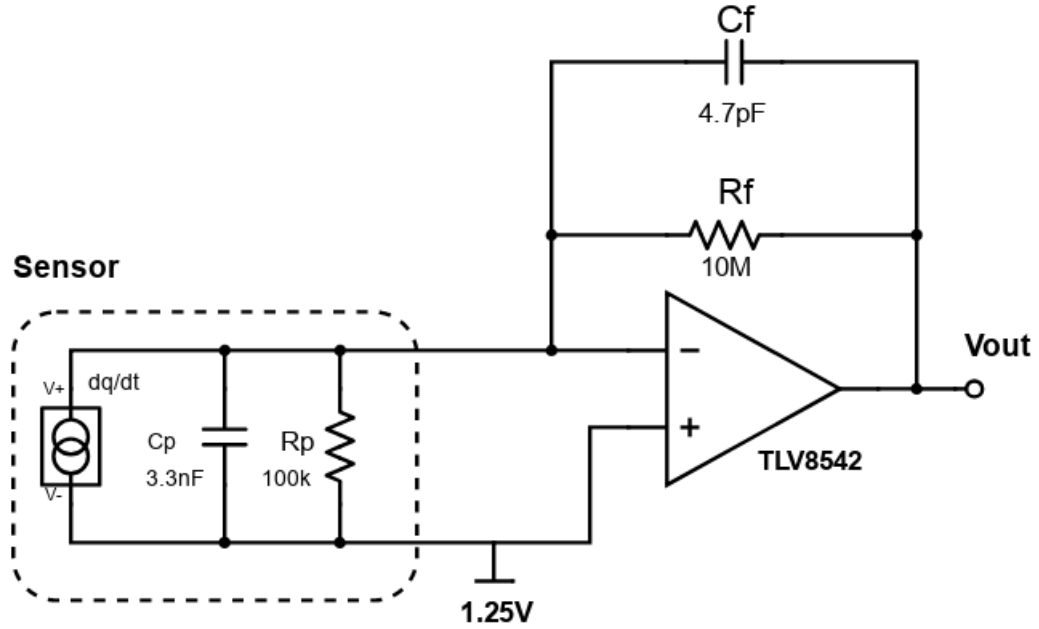


Figure 2.5: Charge Amplifier

The gain of the amplifier is determined by the capacitance of C_f :

$$V_{out} = -\frac{Q_o}{C_f} \quad (2.1)$$

$$G = \frac{V_{out}}{Q_o} = -\frac{1}{C_f}$$

So, for a -227pC/mV gain:

$$-227 \frac{\text{pC}}{\text{mV}} = -\frac{1}{C_f}$$

$$C_f = \frac{1}{227} \times 10^{-9} \text{F} = 4.405 \times 10^{-12} \text{F} \approx 4.47\text{pF}$$

Instead, for R_f we consider the current:

$$R_f = \frac{V_{out_{max}} - V_{out_{min}}}{I_{max}}$$

Let, I_{max} be 100nA :

$$Rf = \frac{2.5V - 0V}{100nA}$$

$$Rf = 25M \rightarrow 10M$$

The RC circuit generates a low pass response with a pole at $\omega = \frac{1}{RC}$

$$fc = \frac{1}{2\pi RC}$$

As this low pass frequency is much higher than the design frequency, or in other words, $fc = 33.86\text{KHz} \gg fc1 = 482\text{Hz}$, the low pass effects can be deprecated.

2.4.1 Component selection

A first Op Amp selection was done taking into account of several parameters, such as input bias current, voltage offset and GBW. For the first prototype the Texas Instruments LMP7712 was chosen.

Op Amp	Supply Voltage	Offset Voltage(max) at 25°C
AD8606	2.7 - 5V	65uV
LTC6268	3.1 - 5.25V	250uV
LTC6081	2.7 - 5.5V	70uV
TLV2771	2.5 - 5.5V	360uV
LMP7721	1.8 - 5.5V	180uV
OPAx320-Q1	1.8 - 5.5V	150uV
LMC6081	4.5 - 15V	350uV
MAX44242	2.7 - 20V	800uV

Table 2.1: Op amp comparison table 1

Op Amp	Offset voltage drift (max)	Supply Current(max)
AD8606	6uV/°C	1.2mA
LTC6268	4uV/°C	18mA
LTC608	0.8uV/°C	460uA
TLV2771	not specified, typ 2uV/°C	2mA
LMP7721	-4uV/°C	1.95mA
OPAx320-Q1	5uV/°C	1.7mA
LMC6081	not specified, typ 1uV/°C	750uA
MAX44242	2.5uV/°C	1.8mA

Table 2.2: Op amp comparison table 2

Op Amp	Input bias Current(max) at 25°C	GBW (min)
AD8606	1pA	10MHz
LTC6268	20fA	400MHz
LTC608	60pA	1.5MHz
TLV2771	100pA	4.9MHz
LMP7721	20fA	15MHz
OPAx320-Q1	0.9pA	20MHz
LMC6081	4pA	1.3MHz
MAX44242	0.5pA	10MHz

Table 2.3: Op amp comparison table 3

Op Amp	PSRR (min)	CMRR (min)	THD
AD8606	70dB	60dB	-86dB
LTC6268	75dB	52dB	-79.6dB
LTC608	96dB	86dB	-90dB
TLV2771	70dB	60dB	-86dB
LMP7721	80dB	80dB	-90dB
OPAx320-Q1	103dB	96dB	-106dB
LMC6081	71dB	63dB	-80dB
MAX44242	100dB	90dB	-124dB

Table 2.4: Op amp comparison table 4

Op Amp	Noise		
	0.1 to 10Hz	1KHz	10KHz
AD8606	3.5uVp-p	12nV/sqrt(Hz)	6.5nV/sqrt(Hz)
LTC6268	13uVp-p	not specified	not specified
LTC6081	1.3uVp-p	13nV/sqrt(Hz)	not specified
TLV2771	0.86uVp-p	17nV/sqrt(Hz)	12nV/sqrt(Hz)
LMP7721	not specified	7nV/sqrt(Hz)	not specified
OPAx320-Q1	2.8uVp-p	8.5nV/sqrt(Hz)	7nV/sqrt(Hz)
LMC6081	not specified	22 nV/sqrt(Hz)	not specified
MAX44242	1.6uVp-p	5nV/sqrt(Hz)	not specified

Table 2.5: Op amp comparison table 5

As being one of the most sensible stages, a single layer PCB was made in order to limit charge leakage, stray capacitance and noise.

It was designed with Altium designer¹⁷ and then etched with the acid method with the following design rules:

- One layer PCB
- No vias
- Minimum hole diameter = 0.6mm/ 23.62mils
- Track Clearance = 20mils
- Pitch = 50mils

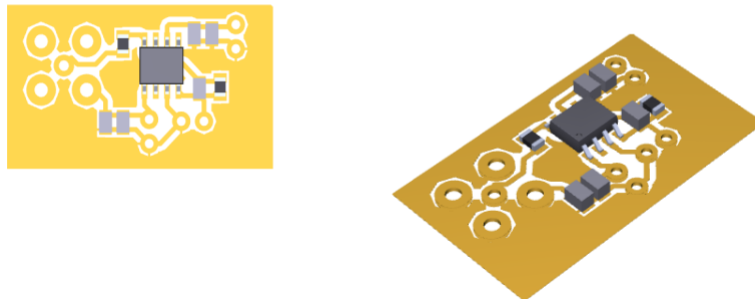


Figure 2.6: PCB 3D View

Once the circuit was characterized and tested a second selection was done with a low power aim. Texas instruments TLV854x was chosen with a very low maximum quiescent current of 640nA.

Device	GBW	Supply current/Op Amp (max)
MAX40006	300KHz	5uA
TSV71/2/4)	120KHz	14uA
SLG88103	10KHz	550nA
HT9274	100KHz	5uA
TSU111	11KHz	1.2uA
MAX40007	15KHz	0.9uA
TLV8544	8KHz	640nA

Table 2.6: Op amp comparison table 6

Device	Supply Voltage	Input bias current(max at 25°C)
MAX40006	1.7-5.5V	20pA
TSV71/2/4)	1.5-5.5V	10pA
SLG88103	1.6-36V	4pA
HT9274	1.6-5.5V	150pA
TSU111	1.5-5.5V	10pA
MAX40007	1.7-5.5V	100pA
TLV8544	1.7-5.5V	100fA (typ)

Table 2.7: Op amp comparison table 7

Device	Package	P/opAmp
MAX40006	0.73mm x 1.07mm(WLP)/3mm x 3mm	12.5uW
TSV71/2/4)	2mm x 1.25mm/2mm x 2mm /3mm x 3mm	35uW
SLG88103	2mm x 2mm /2mm x 3.5mm	1.375uA
HT9274	6mm x 8.65mm	12.5uW
TSU111	2mm x 1.25mm/3mm x 5mm/5mm x 6.9mm	3uW
MAX40007	1.1mm x 0.76mm	2.25uW
TLV8544	8.75mm x 6.2mm	1.6uW

Table 2.8: Op amp comparison table 8

2.5 Low Pass Filter

A second order Chebyshev, Sallen-Key, low pass filter was implemented with a cut off frequency of 482Hz as it was requested. This configuration was chosen because the performance of the op amp has a minor influence on the performance of the filter.

The characteristics of the filter are:

- Cut off frequency (f_c) = 482Hz
- Stop Band frequency (f_s)= 4.82kHz
- Pass band Gain (A_p)= 0dB
- Stop band Gain (A_s)= -40dB
- Pass band Ripple (R_p)= 0.01dB
- Roll-off = -40dB/dec

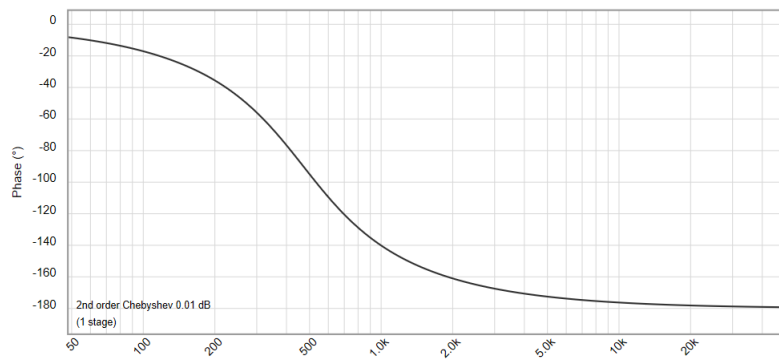
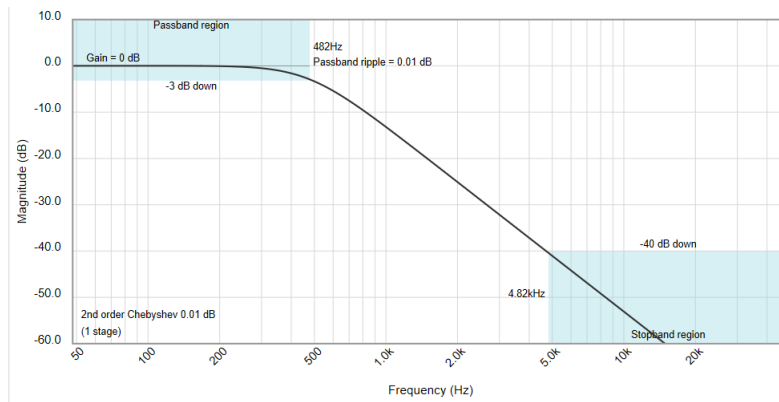


Figure 2.7: Low Pass Frequency Response

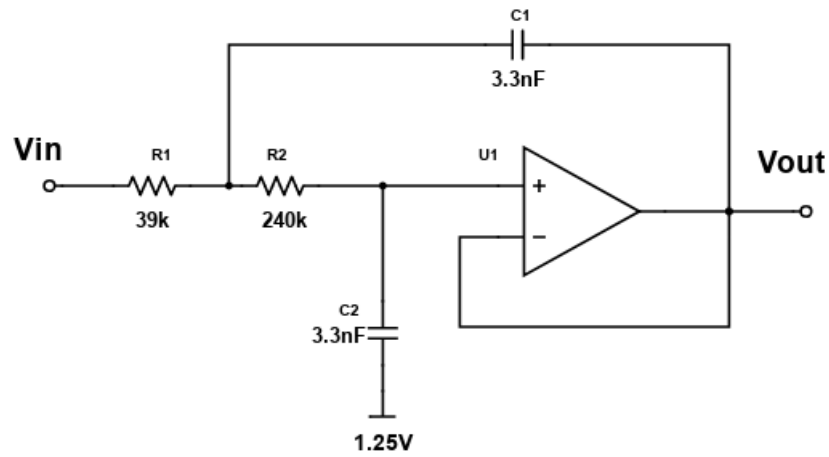


Figure 2.8: Low Pass Filter

Once the circuit was tested there was a 50Hz component interference. So, another filter was proposed by analysing the frequency spectrum of the pulse wave at the radial and carotid artery. The signals were taken from the pulse wave data base from Charlton P.H., Mariscal Harana, J., Vennin, S., Li, Y., Chowienczyk, P. Alastruey, J., “Modelling arterial pulse waves in healthy ageing: a database for in silico evaluation of haemodynamics and pulse wave indices,” *AJP Hear. Circ. Physiol.*, [in press], 2019.

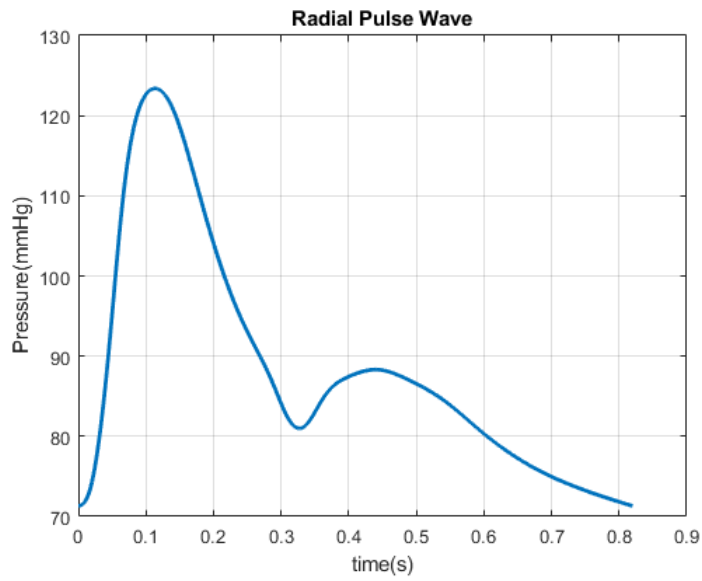


Figure 2.9: Radial Pulse Wave

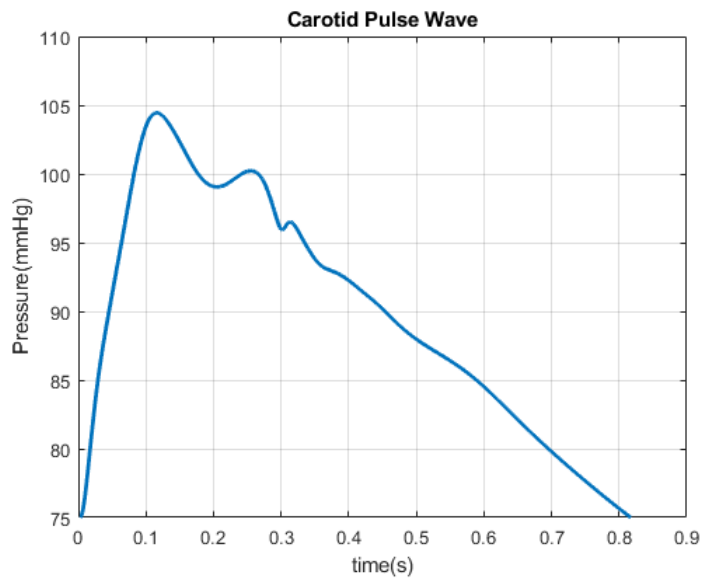


Figure 2.10: Carotid Pulse Wave

Accordingly to the frequency analysis, the signals fundamental frequency corresponds to the hearts rate while 2 to 10 harmonics can be considered for a more precise acquisition. The normalized power spectrum density of both

signals was estimated with Welch's method applying a 256 sample window on a 1 second recording, thus, with a resolution of 1Hz.

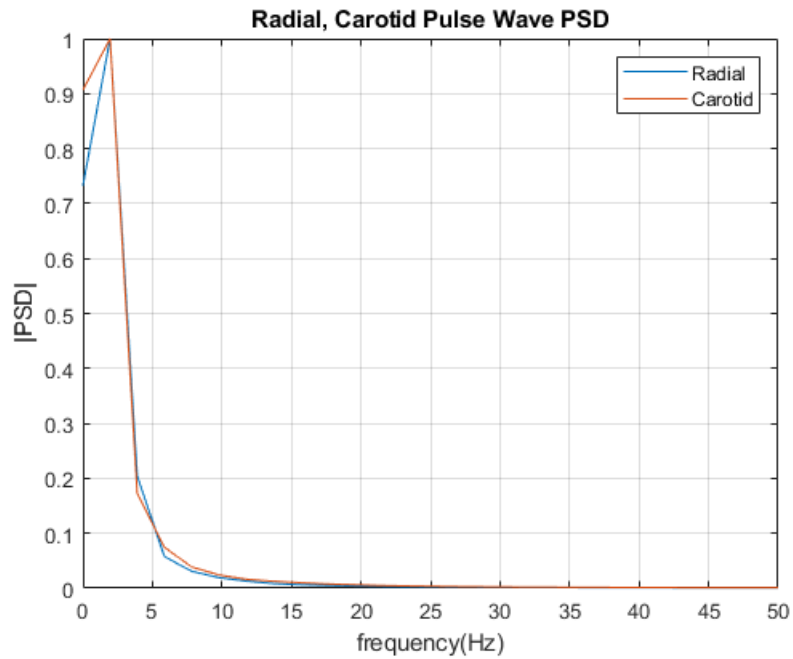


Figure 2.11: Carotid and Radial PSD

As heart rate can be calculated as $220 - 0.7 \text{ patients age}$, we consider a maximum of 220 bpm. This means a 3.67Hz for the fundamental and 36.7Hz for 10 harmonics.

Similar to the previous one, the characteristics of the new filter are:

- Cut off frequency (f_c) = 36.7Hz
- Stop Band frequency (f_s)= 367Hz
- Pass band Gain (A_p)= 0dB
- Stop band Gain (A_s)= -40dB
- Pass band Ripple (R_p)= 0.01dB
- Roll-off = -40dB/dec

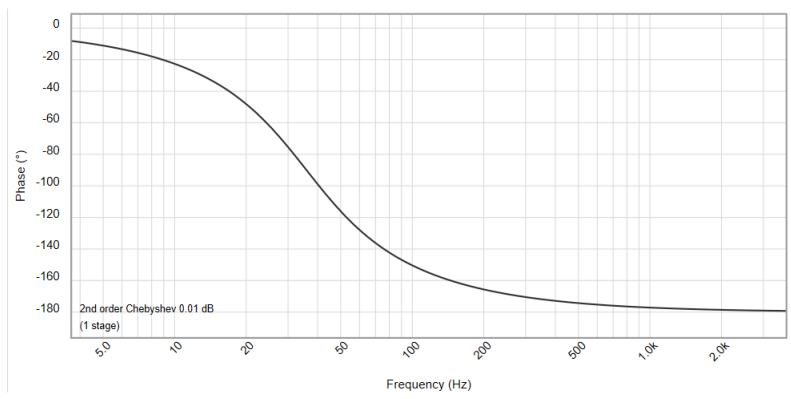
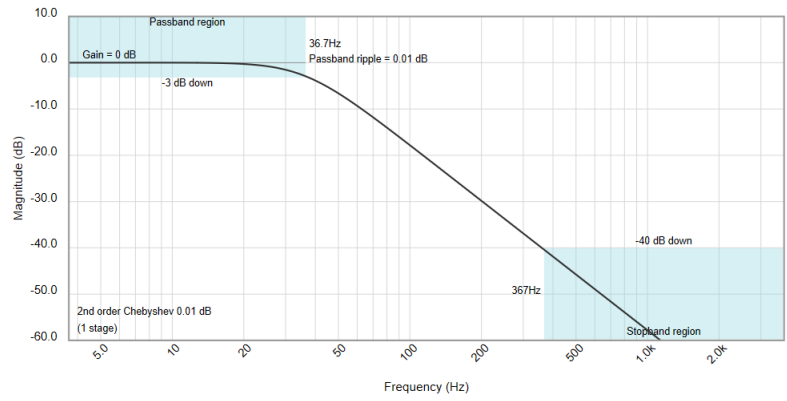


Figure 2.12: Low Pass Frequency Response

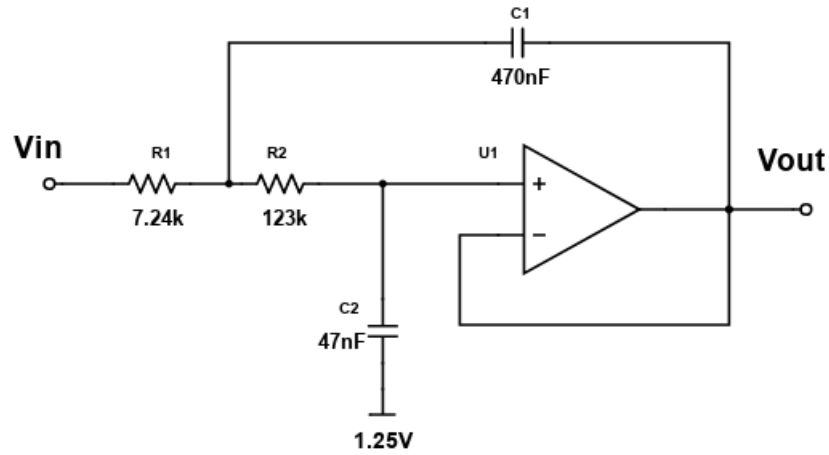


Figure 2.13: Low Pass Filter

2.6 High Pass Filter

A second order Chebyshev, Sallen-Key, high pass filter was implemented with a cut off frequency of 0.5Hz.

The characteristics of the filter are:

- Cut off frequency (f_c) = 0.5Hz
- Stop Band frequency (f_s) = 500mHz
- Pass band Gain (A_p) = 0dB
- Stop band Gain (A_s) = -40dB
- Pass band Ripple (R_p) = 0.01dB
- Roll-off = 40dB/dec

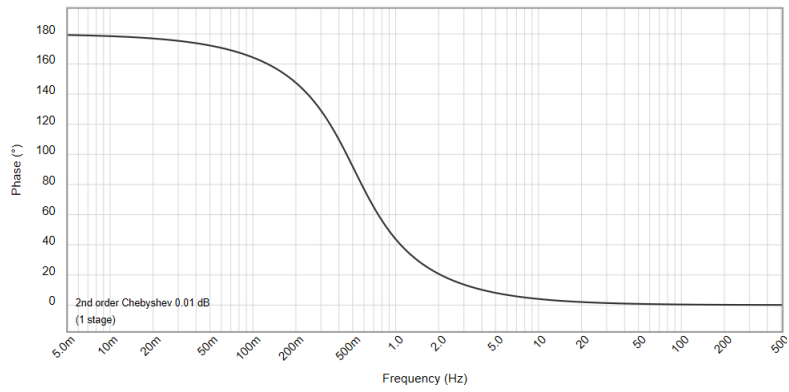
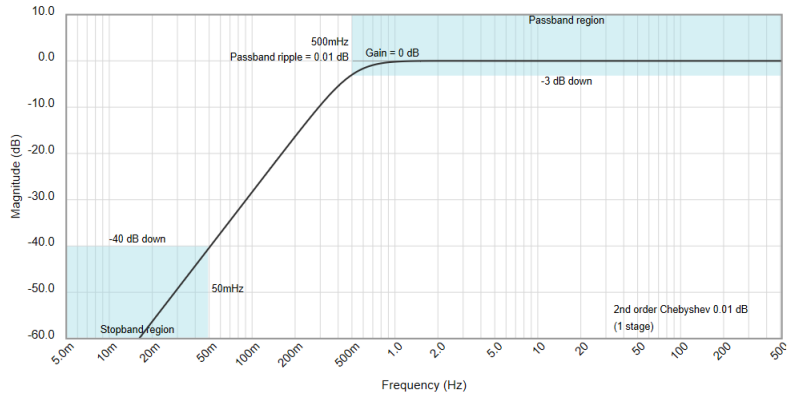


Figure 2.14: High Pass Frequency Response

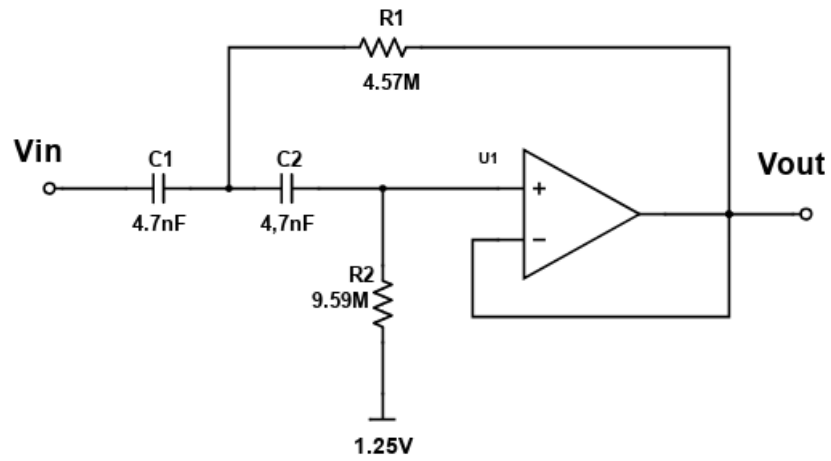


Figure 2.15: High Pass Filter

2.7 Band Pass Filter

Accordingly, we will have two Band Pass final responses:

- $f_1 = 0.5\text{Hz}$
- $f_2 = 482\text{Hz}$
- $f_0 = 15.52\text{Hz}$
- $Q = 0.032$

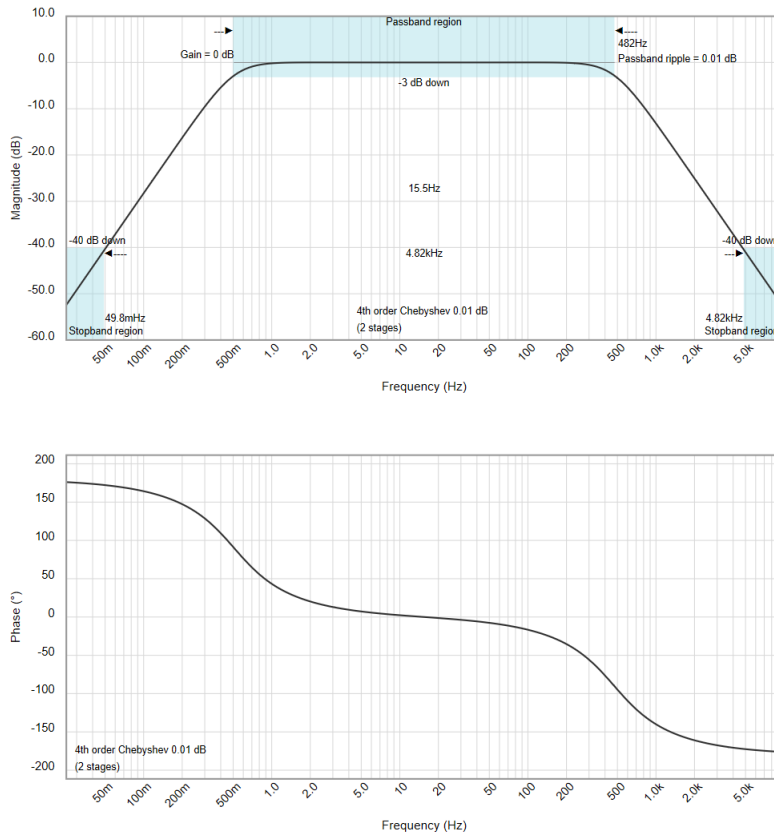


Figure 2.16: Band Pass Frequency Response

And the second one:

- $f_1 = 0.5\text{Hz}$
- $f_2 = 36,7\text{Hz}$
- $f_0 = 4.28\text{Hz}$
- $Q = 0.12$

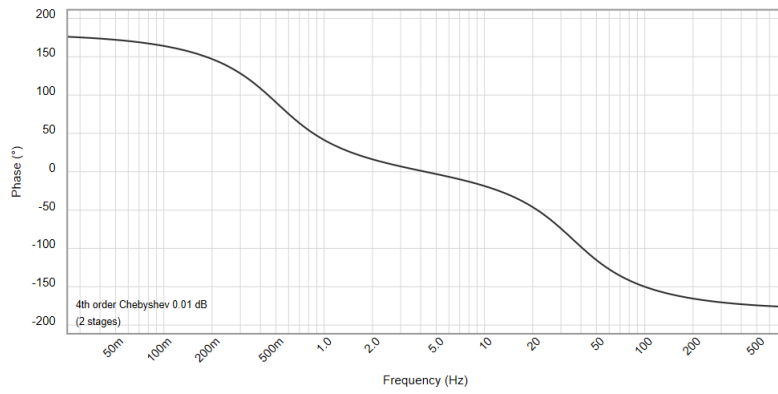
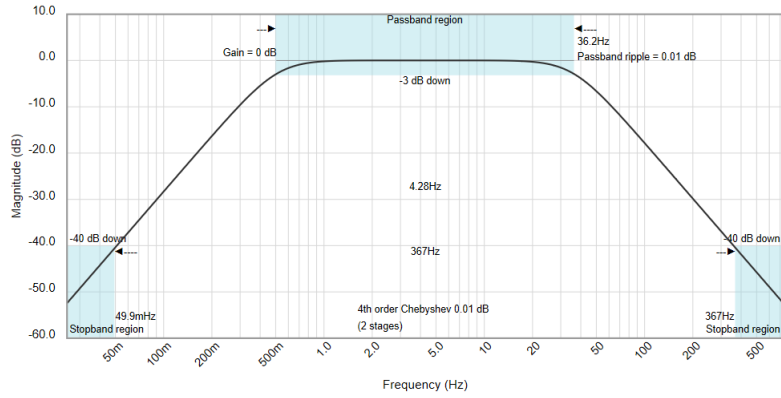


Figure 2.17: Band Pass Frequency Response

2.8 Microcontroller

Next, the digital system design started with selection of an adequate microcontroller by considering Bluetooth, ADC, packaging and power consumption features.

Bluetooth				
Device	Tx Power	Rx sensitivity	Data Rate	antenna
nRF52840	-20 to 8dBm	-95dBm	2Mbps	balun incorporated
Apollo3	-20 to 4dBm	-94dBm	1Mbps	balun incorporated
CC2640R2F	-20 to 5dBm	-91dBm	2Mbps	balun incorporated
DA14580	-20 to 0dBm	-93dBm	1Mbps	single wire antenna
QN908x	-20 to 2dBm	-95dBm	2Mbps	balun incorporated
PSoC6	-20 to 4dBm	-92dBm	1Mbps	integrated balun

Table 2.9: BLE MCU comparison

Core			
Device	Type	Architecture	Clock
nRF52840	Cortex M4	32bit	64MHz
Apollo3	Cortex M4	32bit	48MHz
CC2640R2F	Cortex M3	16bit	48MHz
DA14580	Cortex M0	32bit	16MHz
QN908x	Cortex M0	32bit	32MHz
PSoC6	Cortex M4 + M0	32bit	32MHz

Table 2.10: Core Architecture MCU comparison

Power Consumption			
Device	Active Mode	Sleep Mode	Wake up time
nRF52840	52uA/MHz	1.5uA	3us
Apollo3	41uA/MHz	1uA	15us
CC2640R2F	61uA/MHz	1.1uA	14us
DA14580	40uA/MHz	0.6uA	1.2ms
QN908x	63uA/MHz	750uA	10us
PSoC6	22uA/MHz - 15uA/MHz	7uA	25us

Table 2.11: Power Consumption MCU comparison

ADC		
Device	Resolution	Sample rate
nRF52840	12bit	200ksps
Apollo3	14bit	1.2Msps
CC2640R2F	12bit	200ksps
DA14580	12bit	1Msps
QN908x	16bit	32ksps
PSoC6	16bit	32ksps

Table 2.12: ADC MCU comparison

The low power Ambiq Micro Apollo 3 microcontroller was chosen with some of the features:

- active power consumption: 6uA/MHz
- 14bit ADC with 1Msps
- BLE module



Figure 2.18: Apollo3 Evaluation Board

The program was developed with FreeRTOS kernel allowing to manage a real time threading operative system in order to optimize the code and the performance

2.8.1 ADC

The Apollo3 includes a 15 channel, 14 bit successive approximation Analogue to Digital Converter (ADC) module with a temperature integrated

sensor and battery control. The system implements a CPU free averaging unit with 8 different slots allowing to compute the mean value of the scansions automatically by the hardware and presents several power modes minimizing power consumption.

Also, there are other key features such as a window comparator for monitoring voltages excursions and DMA capability for storing measurements results while rising MCU sleep time. However, on this work the principal features considerer where the high resolution, the low power consumption and the hardware average module.

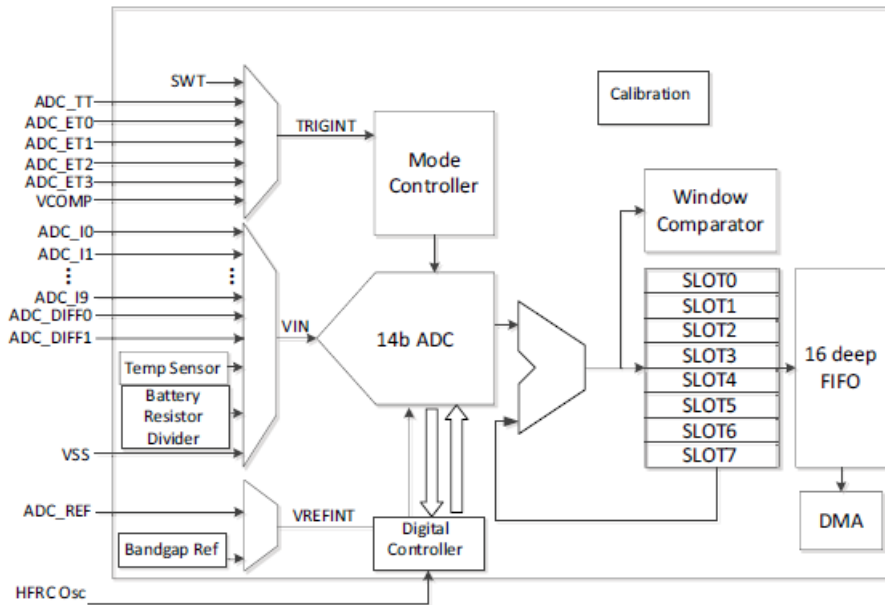


Figure 2.19: ADC block diagram

First, the module must be powered on and enabled. Once its done, the configuration parameters can be set. While resolution can be set to 14, 12, 10 or 8 bit precision, 14 bit is chosen for the higher precision and for the the internal voltage reference setted, at 2V, this means a step of:

$$\frac{2V}{2^{14} - 1} \approx 122.06\mu V$$

Then, the module's power mode is set to LOW POWER MODE 1 in which all ADC circuitry and clocks are powered off between sample scans. This

means the lower power consumption, however a 50us delay is required for the reference buffer to stabilize. Due to relatively low frequency of the signal of interest, this is magnitude order of the Hz, the 50us delay is deprecated.

As one sensor is used, channel 0 is selected for conversion and with the scope of maximum reduction of noise on the measurements, the average of 128 consecutive scans was set. Accordingly, the conversion complete interrupt was set.

In summary, the configuration of the ADC was:

- 14 bit precision
- Clk Source = High Frequency Clock / 2
- 128 average
- Software trigger
- Low Power mode 1
- Single Scan

2.8.2 BLE

The Apollo3 Blue MCU includes a low power Bluetooth low energy subsystem. The BLE controller and host can be configured to support up to seven simultaneous connections on chip revision A1 (4 on chip revision B0). Secure connections and extended packet length are also supported.

The BLE subsystem contains a 2.4 GHz RF transceiver, modem, baseband and 32-bit processor. It supports an external 32 MHz crystal clock source as well as an internal 32 MHz RC oscillator clock source.

The 32 MHz crystal is required as the frequency reference for the radio and also as the main clock source for the controller blocks. The internal 32 MHz RC can be used as a clock source for the RF processor if the requirements allow for lower precision and lower power operation. Driving an active clock into BLE crystal pins is not supported, as the crystal pins do not support active components. The BLE subsystem provides a Host Controller Interface (HCI) to the host

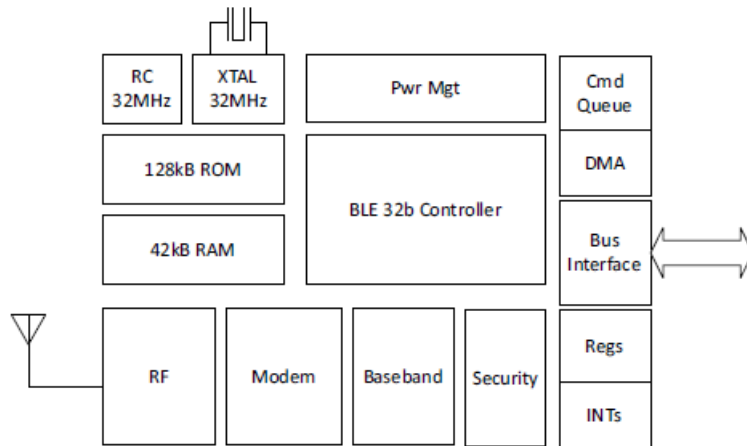


Figure 2.20: BLE module block diagram

Cordio Stack

The Ambiq Apollo3 microcontroller uses ARM's Cordio Stack software system. It is a specialized integrated software that includes a complete protocol stack solution for Bluetooth LE devices and profiles with sample applications for simplified development.

The Cordio stack holds all the necessary protocols for developing a Bluetooth system, this is:

- ATT: Attribute protocol
- SMP: Security manager protocol
- L2C: L2CAP protocol
- HCI: Host controller interface protocol
- DM: Device manager protocol

2.8.3 Deep Sleep

In SYS Deep Sleep Mode 1, this is a deep low power state for the MCU. In this mode, SRAM is in retention (capacity controlled by software), cache memory is powered down, Flash memory is in power down, HFRC is on, main core power domain is off but peripheral power domains can be on. CPU is in Deep Sleep. Core logic state is retained. This state can be entered if the

latency to warm up the cache can be tolerated. This could be an extended wait for peripheral communication event.

2.8.4 Firmware

The firmware consists in a big block of code containing all Cordio stack files that allows the Bluetooth module configuration and operation and the main program in which the FreeRTOS kernel manages ADC, deep sleep and radio tasks. For debugging, one of the on board leds is turned on when the ADC starts due to a on boards button press. Another press means stops the ADC and turns off the led, allowing to test control.

In the main program, some configurations for the system are done. Thus, the systems clock frequency is set to 48MHz while the cache configuration is set to default and the board is set for low power function. Then, task creation and scheduling starts leading to the application to run.

First, before the creation of the tasks and the initialization of the scheduler the interrupt priority must be defined. The GPIO interrupt for the button has to be setted and once is done all the tasks are created.

There are three tasks, the setup task, the radio task and the ADC task. In the setup task all the peripherals are configured as the GPIOs for the button and the led where each initialization is called as a function. Once all peripherals are ready this task is suspended. The ADC task triggers the module each $20\mu s$ for the scansion if it is enabled. When the button is pressed, the ADC is enabled and so its conversion interrupt. Thus, after 128 scansions the conversion interrupt service routine is called and the value is passed to a buffer. In contrast, if the button is pressed again the ADC will be disabled. However, in the idle task of the rtos the MCU enters to deepsleep mode and as a result, when it wakes up the ADC must be configured again and its initialization function is called.

Finally, the radio task initializes the stack, configures the BLE subsystem and starts the BLE profile. When the stack is initialized, several processes are done:

- The WSF subsystem starts and the timers are setted.
- A buffer pool for dynamic memory needs is created

- The security service is initialized
- The callback functions for the stack, such as the Device manager, ATT profile or L2CAP controller are setted up

Once the stack is ready the BLE profile starts. In this profile all the BLE configurations for the application are set.

Slave Parameters

- Advertising: advertise with a 5ms interval for 20seconds
- Maximum connections allowed: 1

Security Parameters

- Request bonding and pair without PIN request
- Minimum number of keys is given
- There is not Out of band data
- Once connection is done, check security

Connection Update Parameters

- Update connection after 3 seconds of no activity
- Connection interval is set to 800 and 1000ms in intervals of 1.25ms
- Latency is set to zero, so slave and master share the same connection intervals
- Supervision time out is set to 5 seconds. If a connection is not granted until this period, the connection is finished
- Number of update attempts: 5

Advertising Data

- Flags: limited discovered mode is set
- Tx power: 0dBm
- Device name: 'Fit' (default name)

2.8.5 MATLAB script

In order to test the BLE communication a MATLAB R2019b script receives the data and plots it. It starts scanning the device by its name and stabilises a connection using its address. Once the connection is verified, a heart rate service instance is initialized and the value of the heart rate characteristic is read in a loop. After all data is received a, mV vs time plot opens.

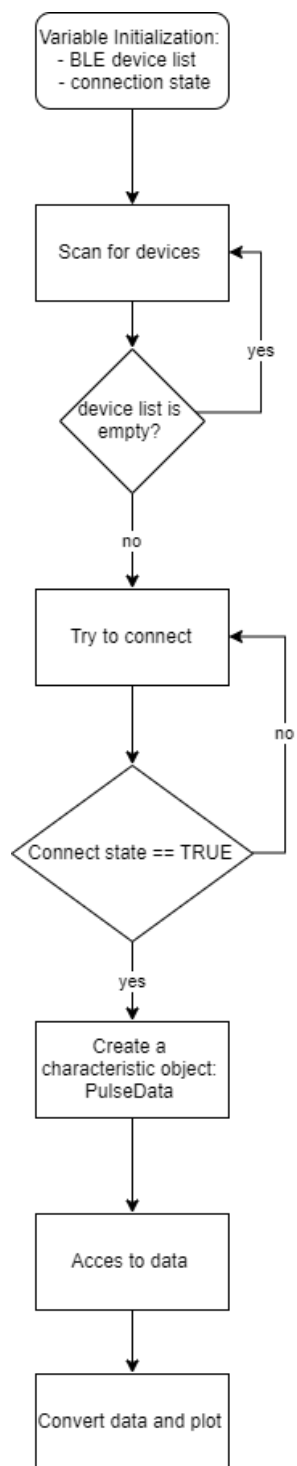


Figure 2.21: MATLAB script flow diagram

Chapter 3

Results

3.1 Charge Amplifier

The charge amplifier was tested with the sensor as input and with a test circuit with a controlled charge injected by a capacitor.

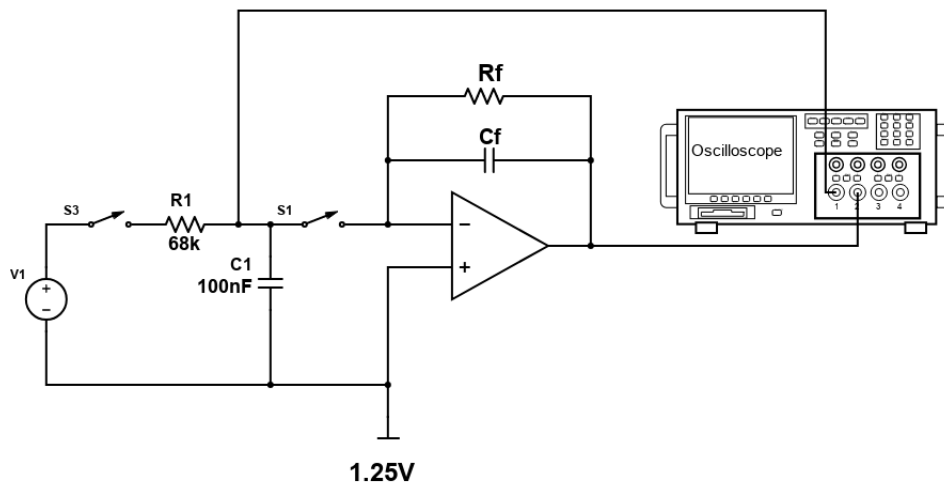


Figure 3.1: Test Circuit

The measured Voltag

Then, the sensor was excited with an impulse in order to determine signal to noise ratio

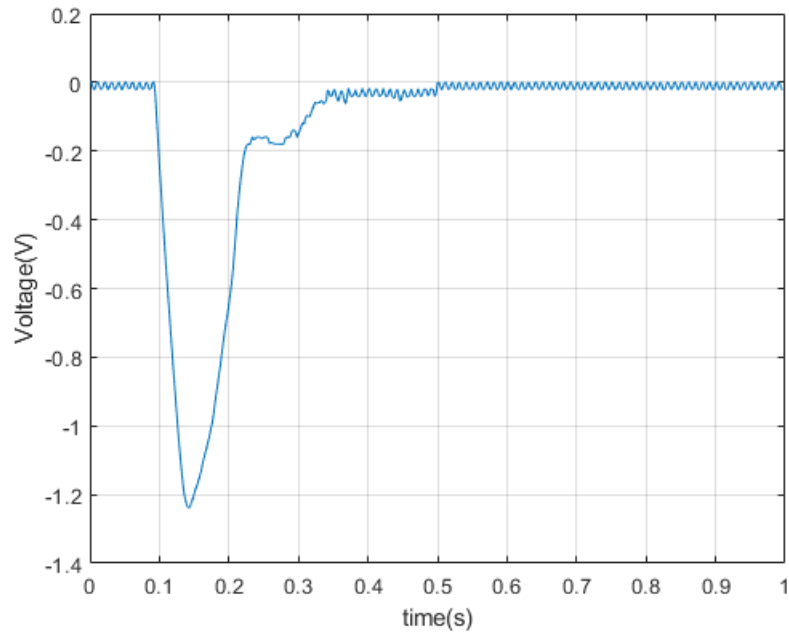


Figure 3.2: Impulse

Considering:

$$Out(t) = signal(t) + noise(t)$$

All samples from 0.1s to 0.35s are considered as signal and the rest of samples from 0.35s to 1s is considered noise. Accordingly, signal to noise ratio is calculated as:

$$SNR_{db} = 20 \log_{10} \left(\frac{\sigma_{signal}}{\sigma_{noise}} \right)$$

$$SNR = 76.89 \text{dB}$$

3.2 Low Pass Filter

First, the components value were measured with a Fluke 179 True-RMS Digital Multimeter:

- R1 = 7.49K
- R2 = 120.5K
- C1 = 452nF

- $C2 = 49\text{nF}$

So, theoretically:

$$f_c = \frac{1}{2\pi\sqrt{R1R2C1C2}} = 35.59\text{Hz}$$

Then, a frequency sweep was done from 1Hz to 30Hz with a 5Hz step between samples with a 100mV Vpp sinusoidal wave as input. From this point, the resolution was augmented to 1Hz between 30 to 35Hz. Finally, 40Hz and 330Hz were measured given the resulting Bode plot. The resulting f_c equals 33Hz.

As,

$$H(s) = \frac{41650}{s^2 + 2741s + 41650}$$

$$w_0 = 2\pi f_c = 207.345 \frac{\text{rad}}{\text{s}}$$

and,

$$2741s = \frac{w_0 s}{Q}$$

then,

$$Q = \frac{w_0}{2741} = 0.0825$$

On the other hand, the 50Hz component is dramatically reduced after the filter application while signal integrity is maintained.

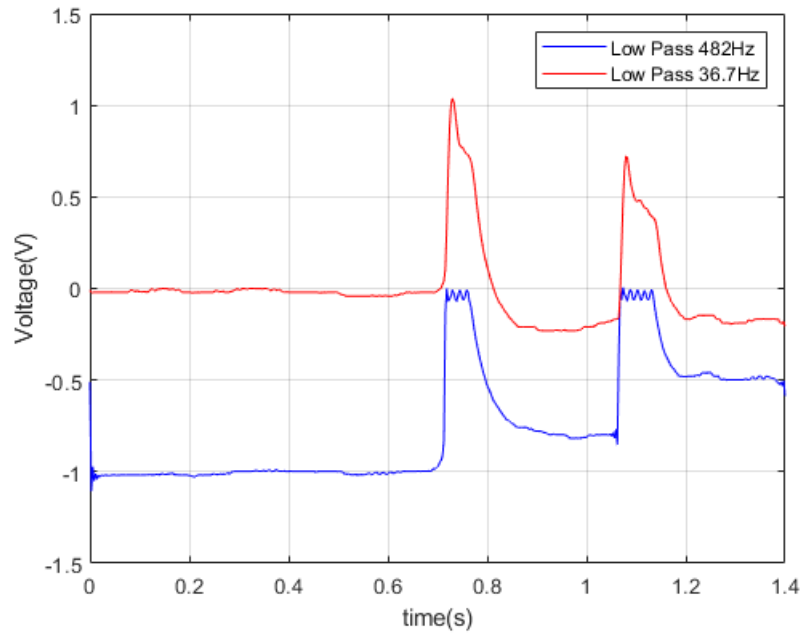


Figure 3.3: Low Pass response comparative

3.3 High Pass Filter

- $C1 = 49\text{nF}$
- $C2 = 49\text{nF}$
- $R1 = 4.708\text{M}$
- $R2 = 10.22\text{M}$

So, theoretically:

$$f_c = \frac{1}{2\pi\sqrt{R1R2C1C2}} = 0.468\text{Hz}$$

Then, a frequency sweep was done from 0.5Hz to 1Hz with a 0.1Hz step between samples and then 0.05Hz were measured.

The resulting f_c equals 0.5Hz.

Frequency sweep						
f(Hz)	Vin(mV)	Vout(mV)	phase	G	Gdb	
0,05	99,970	1,53	180	0,01530459	-36,3035652	
0,5	99,970	70,85	90	0,70871261	-2,99059675	
0,6	99,970	81,48	64,8	0,81504451	-1,77637344	
0,7	99,970	90,34	39,6	0,9036711	-0,87979212	
0,8	99,970	92,11	32,4	0,92137641	-0,7112582	
0,9	99,970	93,88	28,8	0,93908172	-0,54593222	
1	99,970	95,65	18	0,95678704	-0,38369435	
5	99,970	99,19	3,6	0,99219766	-0,06803604	
10	99,970	104,5	-54	1,04531359	0,38493197	
15	99,970	111,5	-57,6	1,1153346	0,94810351	
20	99,970	115,1	-73,8	1,1513454	1,22411263	
25	99,970	102,7	-90	1,02730819	0,23401503	
30	99,970	81,48	-93,6	0,81504451	-1,77637344	
31	99,970	77,94	-90	0,77963389	-2,16218581	
32	99,970	72,62	-86,4	0,72641793	-2,77626895	
33	99,970	69,68	-93,6	0,6970091	-3,135231	
34	99,970	65,54	-86,4	0,65559668	-3,6672651	
35	99,970	61,99	-100,8	0,62008603	-4,15096112	
40	99,970	47,82	-100,8	0,4783435	-6,40520241	
330	99,970	2,91	-180	0,02910873	-30,7195341	

3.4 Band Pass Filter

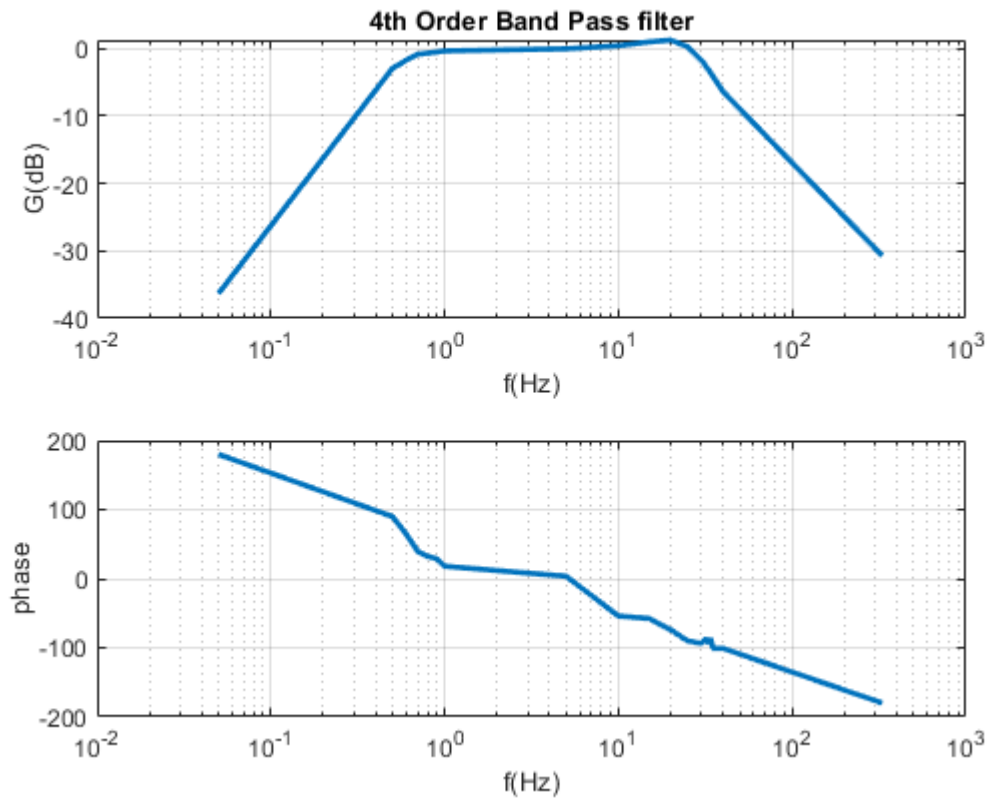


Figure 3.4: Band Pass Filter - Measured

with:

- $f_1 = 0.5\text{Hz}$; -2.99dB
- $f_2 = 33\text{Hz}$; -3.13dB
- $f_c = 4.06\text{Hz}$
- $Q = 0.125$

3.5 ADC Sampling

The sampling rate of the ADC is directly legated with the maximum frequency of the system. As Nyquist theorem evidences, the sampling frequency

must be at least twice of the maximum frequency in order to avoid aliasing phenomena in the conversion.

In the system:

$$f_{max} = 36.7Hz$$

if

$$f_{sampling} = 2f_{nyq} = f_{max}$$

then,

$$f_{sampling} = 73.4Hz$$

As a result, $f_{sampling}$ must be at least 73.4Hz for a correct sampling process.

Considering:

$$128 \times samples \times 70us = 1_{conv} = 8.96ms$$

$$f_{sampling} = \frac{1}{8.96ms} = 111.607Hz > 73.4Hz$$

In order to verify the correct sampling, the ADC was excited with an external DAC that generates a periodic sine wave of 100 samples for increasing frequencies. Then, normalized cross correlation between the measured signal and a synthesized wave was calculated for validation of the sampling.

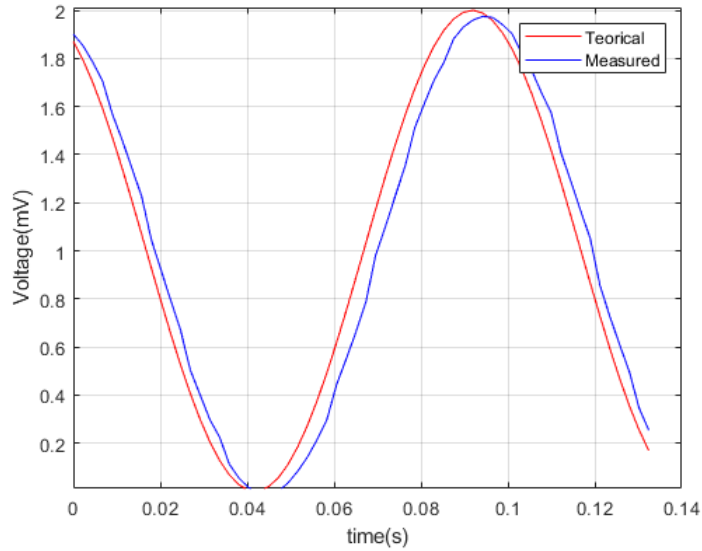


Figure 3.5: Sine Wave vs ADC Wave

f(Hz)	Cross Correlation (%)
1	99.8
10	96.663
20	95
36.7	80.3
50	67
100	68.3

Table 3.1: ADC sampling performance

3.5.1 Power Consumption

First, the analog overall idle consumption is calculated accordingly to the values taken from the manufacturer. Considering the worst case, a 640nA quiescent current per channel is consumed when the device is not active. While implementing 4 op amps the total current must be about $2.56\mu A$. Also, the supply voltage equals 2.5V so, the theoretical power consumption must be:

$$P = I_q \times V_{cc} = 2.56\mu A \times 2.5V = 6.4\mu W$$

As a result, without active load the battery life for the charge amplifier

and the filter would be:

$$\frac{500mAh}{2.56\mu A} = 22.29years$$

Then, a simulation with TINA SPice was done by considering a 1V, 50Ω sinusoidal wave with a 15Hz frequency as input, a high impedance load of 10MΩ and the non ideal parameters of the op Amps:

- Open Loop Gain = 100dB
- Input Resistance = 2MΩ
- Output Resistance = 75Ω
- Input bias current = 100fA
- Input offset voltage = 3.1mV

Obtaining $I_L = 166.66\mu A$, as a result:

$$P = 416.65\mu W$$

and

$$battery\ life = 125days$$

Next, a practical measurement was done by setting up to test the real circuit with the same simulation conditions using a HP Agilent 34401A digital multimeter.

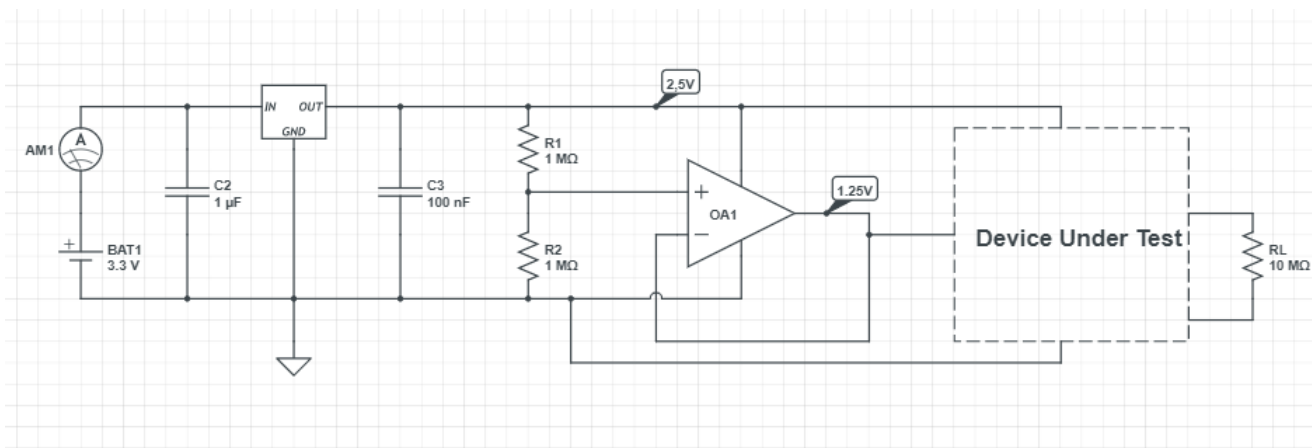


Figure 3.6: Power Measurement Circuit

First, the quiescent current of a single channel was measured obtaining a value of $679\mu A$. Then, the excited circuit was measured giving a a current of $2.20mA$. Accordingly, for the analogue stage:

$$P = V_{cc} \times I_{cc} = 5.5mW$$

and

$$battery\ life = 227hs$$

On the other hand, for the digital system also theoretical power consumption values for a similar to the real scenario were taken from the data sheet of the Apollo3:

	Apollo 3
Clock	On
CPU	WFI
Peripherals	All Idle
Regulator	DC/DC
Sleep	System Deep Sleep mode 2 with 384kB RAM retention: 2.7uA
Active	Flash program run current, Bucks enabled, High Performance Mode: 27uA/MHz (1.29mA at 48MHZ)
BLE	Tx a 0dBm: 3mA
	Rx: 3mA
ADC	- - -
Total	7.29mA

Table 3.2: Power Consumption from data sheet

Then, the current was measured under three different conditions:

- ADC + BLE (connection) = 0.94mA
- ADC + BLE(advertising) = 0.8312mA
- ADC + BLE off = 0.516mA
- Idle = $302\mu A$

In summary, the overall consumption is the sum of the analogue contribute and the digital consumption. Considering the most theoretical demanding performance:

$$P = V_{cc} \times (I_{analog} + I_{digital}) = 2.5V \times (2.2mA + 7.29mA) = 23.725mW$$

and

$$battery\ life = 52.68hs$$

But, considering the measured values with the personalized firmware:

$$P = V_{cc} \times (I_{analog} + I_{digital}) = 2.5V \times (2.2mA + 0.94mA) = 7.85mW$$

and

$$battery\ life = 159.23hs$$

3.5.2 Pulse Wave Recording

Pulse Wave recording was done by placing the sensor on the radial artery at the wrist. For a better transmission of the mechanic wave a standard electrode gel was added between the surface of the sensor and the skin.

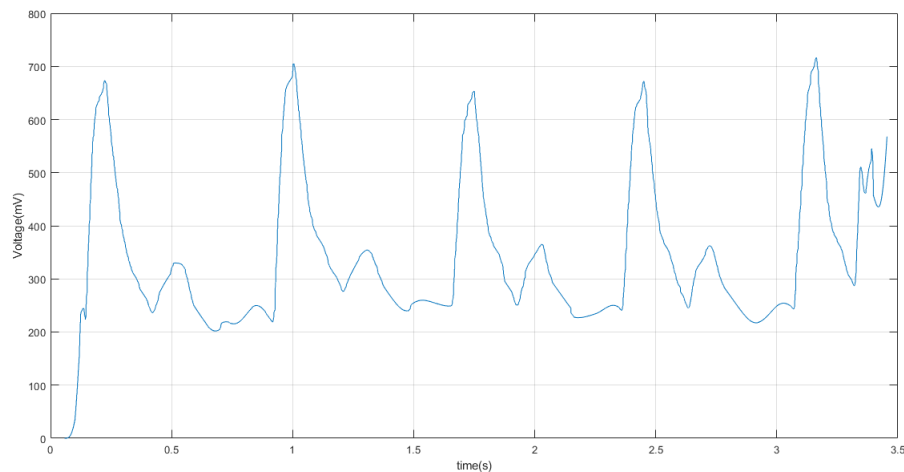


Figure 3.7: Recorded Wave

The normalized power spectrum density of the signal was estimated with Welch's method applying a 256 sample window on a 1 second recording, thus, with a resolution of 1Hz.

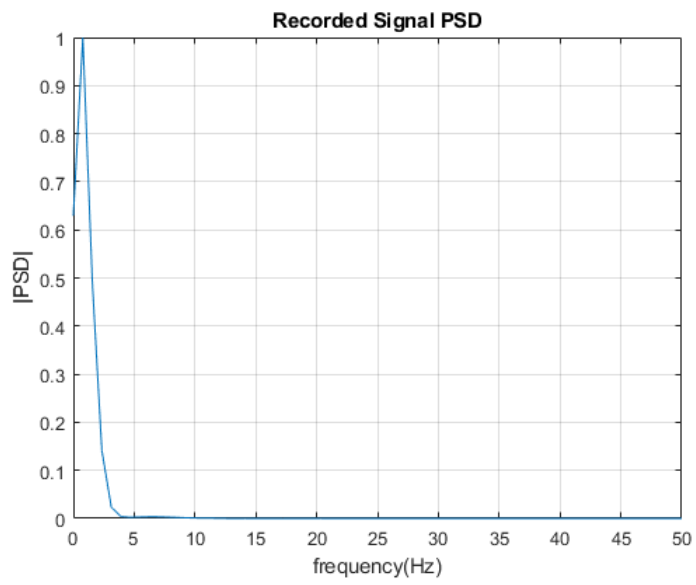


Figure 3.8: Recorded Wave PSD

Chapter 4

Conclusion

In conclusion, a first prototype for the analog and the digital system with a low power and wireless aim was proposed. Regarding the first stage, the cut frequency of the 2nd order low pass filter could be lower as it was tested with the 33Hz filter. However, in some cases irregular heart rate can rise to around 300bpm. If the device is projected for measuring in this conditions implementing this filter could affect the measurement.

Depending on the final application, digital filtering or the addition of a notch filter could be considered for 50Hz removing although the scope of this work was theoretic design and the fabrication of a well defined PCB for all the circuitry should greatly improve the noise performance of the device.

On the other hand the microcontroller stage shows primary a notably low power consumption. Nevertheless, lack of documentation, a well defined software development kit and support for this MCU can render development slow and difficult to integrate. It would be important to consider the compromise of choosing another MCU with a better background at the cost of a higher power consume, at least on an initial stage. Further work must consider development of a smartphone app rather than a MATLAB script, due to BLE technology is designed and conceived for working in this kind of platform.

Finally, the next step could be include a second channel for another sensor allowing to perform real Pulse Wave Analysis, such as velocity wave measuring across correlation of the signals for a more rich information acquisition.

References

- [1] D. Adams. *The Hitchhiker's Guide to the Galaxy*. San Val, 1995.
- [2] Fred J.Taylor Arthur B.Williams. *ELECTRONIC FILTER DESIGN HANDBOOK Fourth Edition*. McGRAW-HILL.
- [3] John E. Hall Ph.D. Arthur C. Guyton, M.D. *TEXTBOOK of Medical Physiology, Eleventh Edition*. Elsevier Inc., 2006.
- [4] Sofia Milaneseyz Diego Marinoyz Francesca Stradolini Paolo Motto Rosyx Federico Pleitavino Danilo Demarchiy Sandro Carrara. *Wearable System for Spinal Cord Injury Rehabilitation with Muscle Fatigue Feedback*. 2018.
- [5] Atmel Corporation. *ATBTLC1000-MR110CA DATA SHEET*. 2016.
- [6] Cypress Semiconductor Corporation. *32-bit ARM® Cortex®-M0+ FM0+ Microcontroller Data Sheet*. 2017.
- [7] Cypress Semiconductor Corporation. *PSoC 63 MCU with Bluetooth LE Data Sheet*. 2019.
- [8] Linear Technology Corporation. *LTC6081/LTC6082 Data Sheet*.
- [9] Linear Technology Corporation. *LTC6268/LTC6269 Data Sheet*.
- [10] Rohit Kumar Cypress Semiconductor Corporation. *AN91162-Creating a BLE Custom Profile*.
- [11] Sergio Cova. *Sensors, Signals and Noise-SE3 Piezoelectric Force Sensors*. 2010.
- [12] L. DOLEŽAL D. KORPAS, J. HÁLEK. *Parameters Describing the Pulse Wave*. *Physiol. Res.*, 2009.
- [13] ANALOG DEVICES. *AD8605/AD8606/AD8608 Data Sheet*.
- [14] Epec. *YOUR LEADING PROVIDER OF HIGH QUALITY FLEX RIGID-FLEX CIRCUITS*.
- [15] Tech Etch. *Flexible Printed Circuits Design Guide*.
- [16] Arnaud Deraemaeker Etienne Balmes. *Modeling structures with piezoelectric materials Theory and SDT Tutorial*. 2019.
- [17] Sergio Franco. *Desig with Operational Amplifiers and Analog Integrated Circuits, third ediction*. Mc Graw Hill, 2001.
- [18] Kistler Group. *Kistler LabAmp Charge Amplifier and Data Acquisition Unit for Dynamic Measurements*. 2019.
- [19] Svein Kristian Esp Hansen. *Design and Experimental Investigation of Charge Amplifiers for Ultrasonic Transducers*. 2014.

- [20] HOLTEK. *HT9274 Quad Micropower Op Amp*. 2019.
- [21] Ambiq Micro Inc. *Apollo3 Blue Datasheet*.
- [22] Ambiq Micro Inc. *AmbiqSuite SDK Getting Started Guide*. 2007.
- [23] Maxim Integrated Products Inc. *MAX40006-Micropower, Rail-to-Rail, 300kHz Op Amp with Shutdown in a Tiny, 6-Bump WLP*. 2018.
- [24] Maxim Integrated Products Inc. *MAX40007-nanoPower Op Amp in Ultra-Tiny WLP and SOT23 Packages*. 2018.
- [25] Maxim Integrated Products Inc. *MAX44242-20V, Low Input Bias-Current, Low-Noise, Dual Op Amplifier*. 2018.
- [26] RIGOL (SUZHOU) TECHNOLOGIES INC. *MSO5000 Series Digital Oscilloscope*. 2018.
- [27] Silicon Laboratories Inc. *UG103.14: Bluetooth® LE Fundamentals*.
- [28] Silicon Laboratories Inc. *How to Pick the Right Microcontroller Based on Low-Power Specifications*. 2013.
- [29] Texas Instruments Incorporated. *TLV277x, TLV277xA- FAMILY OF 2.7-V HIGH SLEW RATE RAIL TO RAIL OUTPUT OPERATIONAL AMPLIFIERS WITH SHUT DOWN*. 2004.
- [30] Texas Instruments Incorporated. *LMC6062 Precision CMOS Dual Micropower Operational Amplifier*. 2013.
- [31] Texas Instruments Incorporated. *LMC6081 Precision CMOS Single Operational Amplifier*. 2013.
- [32] Texas Instruments Incorporated. *LMP7721 3-Femtoampere Input Bias Current Precision Amplifier*. 2014.
- [33] Texas Instruments Incorporated. *OPA320-Q1 Precision, 20-MHz, 0.9-pA, Low-Noise, RRIO, CMOS Operational Amplifier*. 2018.
- [34] Texas Instruments Incorporated. *TLV854x 500-nA, RRIO, Nanopower Operational Amplifiers for Cost-Optimized Systems*. 2018.
- [35] Texas Instruments Incorporated. *CC2640R2F SimpleLink™ Bluetooth® 5.1 Low Energy Wireless MCU*. 2020.
- [36] Texas Instruments Incorporated James Karki. *Signal Conditioning Piezoelectric Sensors*. 2000.
- [37] Trevor Martin. *The Designer's Guide to the Cortex-M Processor Family-A Tutorial Approach*. Elsevier, 2013.

- [38] S. A. PACTITIS. *ACTIVE FILTERS Theory and Design*. CRC Press Taylor Francis Group, 2007.
- [39] Texas Instruments Incorporated Ron Mancini. *So many amplifiers to choose from: Matching amplifiers to applications*. 2005.
- [40] Dialog Semiconductor. *DA14580 Bluetooth Low Energy 4.2 SoC Data Sheet*. 2014.
- [41] NXP Semiconductors. *QN908x Ultra low power Bluetooth 5 system-on-chip solution-Product Data Sheet*. 2018.
- [42] STMicroelectronics. *TSU111, TSU112, TSU114 Datasheet*.
- [43] STMicroelectronics. *TSV711, TSV712, TSV714 Datasheet*.
- [44] STMicroelectronics. *TSV731, TSV732, TSV734 Datasheet*.
- [45] Teledyne Electronic Technologies. *Flexible Circuit Design Guide, Fourth Edition*.
- [46] Silego Technology. *SLG88103/4-Rail to Rail I/O 375 nA/Amp Dual/Quad CMOS Op Amps with Power Down*.
- [47] Tektronix. *Internet of Things: How to Select A Bluetooth Module APPLICATION NOTE*.